P-86

BAW-1436 2487

September 1977

RETURN TO REGULATORY CENTRAL FILES
ROOM 016

ANALYSIS OF CAPSULE OCI-E
DUKE POWER COMPANY
OCONEE NUCLEAR STATION — UNIT 1
— Reactor Vessel Materials Surveillance Program —

— NOTICE —

THE ATTACHED FILES ARE OFFICIAL RECORDS OF THE DIVISION OF DOCUMENT CONTROL. THEY HAVE BEEN CHARGED TO YOU FOR A LIMITED TIME PERIOD AND MUST BE RETURNED TO THE RECORDS FACILITY BRANCH 016. PLEASE DO NOT SEND DOCUMENTS CHARGED OUT THROUGH THE MAIL. REMOVAL OF ANY PAGE(S) FROM DOCUMENT FOR REPRODUCTION MUST BE REFERRED TO FILE PERSONNEL.

DEADLINE RETURN DATE _____

_____ _____

_____ _____

_____ _____

RECORDS FACILITY BRANCH

Babcock & Wilcox

RETURN TO REGULATORY CENTRAL FILES
ROOM 016

7912060695 P

BAW-1436

September 1977

ANALYSIS OF CAPSULE OCI-E
DUKE POWER COMPANY
OCONEE NUCLEAR STATION — UNIT 1

— Reactor Vessel Materials Surveillance Program —

by

A. L. Lowe, Jr., PE
E. T. Chulick
H. S. Palme
C. L. Whitmarsh
C. F. Zurlippe

B&W Contract No. 595-7020-51

BABCOCK & WILCOX
Power Generation Group
Nuclear Power Generation Division
P. O. Box 1260
Lynchburg, Virginia 24505

Babcock & Wilcox

CONTENTS

		Page
1.	INTRODUCTION	1-1
2.	BACKGROUND	2-1
3.	SURVEILLANCE PROGRAM DESCRIPTION	3-1
4.	PREIRRADIATION TESTS	4-1
	4.1. Tensile Tests	4-1
	4.2. Impact Tests	4-1
5.	POSTIRRADIATION TESTS	5-1
	5.1. Thermal Monitors	5-1
	5.2. Chemical Analysis	5-1
	5.3. Tensile Test Results	5-1
	5.4. Charpy V-Notch Impact Test Results	5-2
6.	NEUTRON DOSIMETRY	6-1
	6.1. Introduction	6-1
	6.2. Analytical Approach	6-2
	6.3. Results	6-3
7.	DISCUSSION OF CAPSULE RESULTS	7-1
	7.1. Preirradiation Property Data	7-1
	7.2. Irradiated Property Data	7-1
	7.2.1. Tensile Properties	7-1
	7.2.2. Impact Properties	7-1
8.	DETERMINATION OF RCPB PRESSURE-TEMPERATURE LIMITS	8-1
9.	SUMMARY OF RESULTS	9-1
10.	SURVEILLANCE CAPSULE REMOVAL SCHEDULE	10-1
11.	CERTIFICATION	11-1
12.	REFERENCES	12-1

Contents (Cont'd)

Page

APPENDIXES

A. Reactor Vessel Surveillance Program — Background Data and Information A-1
B. Preirradiation Tensile Data B-1
C. Preirradiation Cha py Impact Data C-1
D. Threshold Detector Information D-1

List of Tables

Table

3-1. Specimens in Surveillance Capsule OCI-E 3-2
3-2. Chemistry and Heat Treatment of Surveillance Materials 3-3
3-3. Chemistry and Heat Treatment of Correlation Material — Heat A-1195-1, A533 Grade B, Class 1 3-4
5-1. Chemistry Data on Unirradiated Oconee 1 RVSP Material 5-2
5-2. Tensile Properties of Capsule OCI-E Base Metal and Weld Metal Irradiated to 1.5×10^{18} nvt 5-3
5-3. Charpy Impact Data for Capsule OCI-E Base Metal Irradiated to 1.5×10^{18} nvt 5-4
5-4. Charpy Impact Data for Capsule OCI-E Weld Metal (WF-112) Irradiated t .5 × 10^{18} nvt 5-5
5-5. Charpy Impa Data for Capsule OCI-E Correlation Monitor Material Irradiated to 1.5×10^{18} nvt 5-5
6-1. Surveillance Capsule Detectors 6-5
6-2. Flux Adjustment Factor 6-5
6-3. Dosimeter Activations After Cycle 2 6-6
6-4. Normalized Flux Spectra, E > 1 MeV 6-7
6-5. Fast Neutron Fluence 6-7
6-6. Predicted Fast Fluence in Pressure Vessel for 10 EFPY 6-8
7-1. Comparison of Tensile Test Results 7-4
7-2. Observed Vs Predicted Changes in Irradiated Charpy Impact Properties 7-5
8-1. Data for Preparation of Pressure-Temperature Limit Curves for Oconee Unit 1, Applicable Through 8 EFPY 8-4
A-1. Surveillance Program Materials Selection Data for Oconee 1 . . . A-3
A-2. Materials and Specimens in Upper Surveillance Capsules OCI-A, OCI-C, and OCI-E A-4
A-3. Materials and Specimens in Lower Surveillance Capsules OCI-B, OCI-D, and OCI-F A-4
B-1. Preirradiation Tensile Properties of Shell Plate Material, Heat C-3265-1 . . . . . B-2
B-2. Preirradiation Tensile Properties of Shell Plate Material, HAZ, Heat C-3265-1 . . . . . B-3
B-3. Preirradiation Tensile Properties of Weld Metal, Weld Qualification No WF112 . . . . . B-4

List of Tables (Cont'd)

Table		Page
C-1.	Preirradiation Charpy Impact Data for Shell Plate Material, Longitudinal Direction, Heat C-3265-1	C-2
C-2.	Preirradiation Charpy Impact Data for Shell Plate Material, Transverse Direction, Heat C-3261-1	C-3
C-3.	Preirradiation Charpy Impact Data for Shell Material, HAZ, Longitudinal Direction, Heat C-3265-1	C-4
C-4.	Preirradiation Charpy Impact Data for Shell Material, HAZ, Transverse Direction, Heat C-3265-1	C-5
C-5.	Preirradiation Charpy Impact Data for Weld Metal, Weld Qualification No. WF 112	C-6
D-1.	Detector Composition and Shielding	D-2
D-2.	Measured Detector Activities After Cycle 1	D-3
D-3.	Measured Detector Activities After Cycle 2	D-4
D-4.	Dosimeter Activation Cross Sections	D-7

List of Figures

Figure		
3-1.	Reactor Vessel Cross Section Showing Surveillance Capsule Locations	3-5
5-1.	Charpy Impact Data From Irradiated Base Metal, Longitudinal Orientation	5-6
5-2.	Charpy Impact Data From Irradiated Base Metal, Transverse Orientation	5-7
5-3.	Charpy Impact Data From Irradiated Base Metal Heat-Affected Zone, Longitudinal Orientation	5-8
5-4.	Charpy Impact Data From Irradiated Weld Metal	5-9
5-5.	Charpy Impact Data From Irradiated Correlation Monitor Material	5-10
6-1.	Predicted Fast Neutron Fluences at Various Locations Through Reactor Vessel Wall for First 10 EFPY	6-9
7-1.	Irradiated Vs Unirradiated Charpy Impact Properties of Base Metal, Longitudinal Orientation	7-6
7-2.	Irradiated Vs Unirradiated Charpy Impact Properties of Base Metal, Transverse Orientation	7-7
7-3.	Irradiated Vs Unirradiated Charpy Impact Properties of Base Metal, Heat-Affected Zone, Longitudinal Orientation	7-8
7-4.	Irradiated Vs Unirradiated Charpy Impact Properties of Weld Metal	7-9
7-5.	Irradiated Vs Unirradiated Charpy Impact Properties of Correlation Monitor Material	7-10
8-1.	Fast Neutron Fluence of Surveillance Capsule Center Compared to Various Locations Through Reactor Vessel Wall for First 10 EFPY	8-5
8-2.	Reactor Vessel Pressure-Temperature Limit Curves for Normal Operation Heatup Applicable for First 8 EFPY	8-6

List of Figures (Cont'd)

Figure		Page
8-3.	Reactor Vessel Pressure-Temperature Limit Curve for Normal Operation - Cooldown Applicable for First 8 EFPY	8-7
8-4.	Reactor Vessel Pressure-Temperature Limit Curve for Inservice Leak and Hydrostatic Tests, Applicable for First 8 EFPY	8-8
A-1.	Location and Identification of Materials Used in Fabrication of Oconee Unit 1 Reactor Pressure Value	A-5
A-2.	Location of Longitudinal Welds in Upper, Lower, and Intermediate Shell Courses	A-6
C-1.	Impact Data From Unirradiated Base Metal A — Longitudinal Orientation	C-7
C-2.	Impact Data From Unirradiated Base Metal A — Transverse Orientation	C-8
C-3.	Impact Data From Unirradiated Base Metal A — HAZ, Longitudinal Orientation	C-9
C-4.	Impact Data From Unirradiated Base Metal A — HAZ, Transverse Orientation	C-10
C-5.	Impact Data From Unirradiated Weld Metal Longitudinal Orientation	C-11
C-6.	Impact Data Unirradiated Correlation Material	C-12

1. INTRODUCTION

This report describes the results of the examination of the second capsule of the Duke Power Company's Oconee Nuclear Station, Unit 1 reactor vessel surveillance program. The first capsule of the program was removed and examined after the first year of operation; the results are reported in BAW-1421.[1]

The objective of the program is to monitor the effects of neutron irradiation on the tensile and impact properties of reactor pressure vessel materials under actual operating conditions. The surveillance program for Oconee 1 was designed and furnished by Babcock & Wilcox as described in BAW-10006A.[2] The program was designed in accordance with E185-66 and was planned to monitor the effects of neutron irradiation on the reactor vessel material for the 40-year design life of the reactor pressure vessel.

The surveillance program for Oconee 1 was not designed in accordance with Appendixes G and H to 10 CFR 50 since the requirements did not exist at the time the program was designed. Because of this difference, at the time the first capsule was removed and specimens tested, additional tests and evaluations were performed to ensure that the requirements of 10 CFR 50, Appendixes G and H were met. The recommendations for the future operation of Oconee 1 after the evaluation of the first capsule complied with these requirements. The future operating limitations established after the evaluation of the second surveillance capsule are also in accordance with the requirement of 10 CFR 50, Appendixes G and H. The recommended operating period was extended from five to eight effective full power years as a result of the second capsule evaluation.

2. BACKGROUND

The ability of the reactor pressure vessel to resist fracture is the primary factor in ensuring the safety of the primary system in light water cooled reactors. The beltline region of the reactor vessel is the most critical region of the vessel because it is exposed to neutron irradiation. The general effects of fast neutron irradiation on the mechanical properties of such low-alloy ferritic steels as SA302B, Code Case 1339, used in the fabrication of the Oconee 1 reactor vessel are well characterized and documented in the literature. The low-alloy ferritic steels used in the beltline region of reactor vessels exhibit an increase in ultimate and yield strength properties with a corresponding decrease in ductility after irradiation. In reactor pressure vessel steels, the most serious mechanical property change is the increase in temperature for the transition from brittle to ductile fracture accompanied by a reduction in the upper shelf impact strength.

Appendix G to 10 CFR 50, "Fracture Toughness Requirements," specifies minimum fracture toughness requirements for the ferritic materials of the pressure-retaining components of the reactor coolant pressure boundary (RCPB) of water-cooled power reactors and provides specific guidelines for determining the pressure-temperature limitations on operation of the RCPB. The toughness and operational requirements are specified to provide adequate safety margins during any condition of normal operation, including anticipated operational occurrences and system hydrostatic tests, to which the pressure boundary may be subjected over its service lifetime. Although the requirements of Appendix G to 10 CFR 50 became effective on August 13, 1973, the requirements are applicable to all boiling and pressurized water-cooled nuclear power reactors, including those under construction or in operation on the effective date.

Appendix H to 10 CFR 50, "Reactor Vessel Materials Surveillance Program Requirements," defines the material surveillance program required to monitor changes in the fracture toughness properties of ferritic materials in the reactor vessel beltline region of water-cooled reactors resulting from exposure

to neutron irradiation and the thermal environment. Fracture toughness test data are obtained from material specimens withdrawn periodically from the reactor vessel. These data will permit determination of the conditions under which the vessel can be operated with adequate safety margins against fracture throughout its service life.

A method for guarding against brittle fracture in reactor pressure vessels is described in Appendix G to the ASME Boiler and Pressure Vessel Code, Section III. This method utilizes fracture mechanics concepts and the reference nil-ductility temperature, RT_{NDT}, which is defined as the greater of the drop weight nil-ductility transition temperature (per ASTM E-208) or the temperature that is 60F below that at which the material exhibits 50 ft-lb and 35 mils lateral expansion. The RT_{NDT} of a given material is used to index that material to a reference stress intensity factor curve (K_{IR} curve), which appears in Appendix G of ASME Section III. The K_{IR} curve is a lower bound of dynamic, static, and crack arrest fracture toughness results obtained from several heats of pressure vessel steel. When a given material is indexed to the K_{IR} curve, allowable stress intensity factors can be obtained for this material as a function of temperature. Allowable operating limits can then be determined using these allowable stress intensity factors.

The RT_{NDT} and, in turn, the operating limits of a nuclear power plant, can be adjusted to account for the effects of radiation on the properties of the reactor vessel materials. The radiation embrittlement and the resultant changes in mechanical properties of a given pressure vessel steel can be monitored by surveillance program in which a surveillance capsule containing prepared specimens of the reactor vessel materials is periodically removed from the operating nuclear reactor and the specimens tested. The increase in the Charpy V-notch 50-ft-lb temperature, or the increase in the 35 mils of lateral expansion temperature, whichever results in the larger temperature shift due to irradiation, is added to the original RT_{NDT} to adjust it for radiation embrittlement. This adjusted RT_{NDT} is used to index the material to the K_{IR} curve, which, in turn is used to set operating limits for the nuclear power plant. These new limits take into account the effects of irradiation on the reactor vessel materials.

3. SURVEILLANCE PROGRAM DESCRIPTION

The surveillance program for Oconee 1 comprises eight surveillance capsules designed to monitor the effects of neutron and thermal environment on the materials of the reactor pressure vessel core region. The capsules, which were inserted into the reactor vessel before initial plant startup, were positioned inside the reactor vessel between the thermal shield and the vessel wall at the locations shown in Figure 3-1. Six of the capsules, placed two in each holder tube, are positioned near the peak axial and azimuthal neutron flux. The remaining two capsules are thermal aging capsules and are placed in an area of essentially zero neutron flux. BAW-10006A includes a full description of capsule locations and design.[1]

Capsule OCI-E was removed during the second refueling shutdown of Oconee 1. This capsule contained Charpy V-notch impact and tensile specimens fabricated of SA302, Gr B Modified Steel, weld metal and correlation steel. The specimen contained in the capsule are described in Table 3-1, and the chemistry and heat treatment of the surveillance material in capsule OCI-E are described in Table 3-2.

The capsule also contained longitudinal Charpy V-notch specimens from correlation material obtained from plate 02 of the USAEC Heavy Section Steel Technology Program. This 12-inch-thick plate of ASTM 533, Grade B, Class 1 steel was produced by the Luken Steel Company (heat A-1195-1) and heat-treated by Combustion Engineering. The chemistry and heat treatment of the correlation material are described in Table 3-3.

All test specimens were machined from the 1/4-thickness location of the plates. Charpy V-notch and tensile specimens from the vessel material were oriented with their longitudinal axes parallel to the principal rolling direction of the plate; the specimens were also oriented transverse to the principal rolling direction. Capsule OCI-E contained dosimeter wires, described as follows:

Dosimeter wire	Shielding
U-Al alloy	Cd-Ag alloy
Np-Al alloy	Cd-Ag alloy
Nickel	Cd-Ag alloy
0.66% Co-Al alloy	Cd
0.66% Co-Al alloy	None
Fe	None

Thermal monitors of low-melting eutectic alloys were included in the capsule. The eutectic alloys and their melting points are as follows:

Alloy	Melting point, F
90% Pb, 5% Ag, 5% Sn	558
97.5% Pb, 2.5% Ag	580
97.5% Pb, 1.5% Ag, 1.0% Sn	588
Lead	621
Cadmium	610

Table 3-1. Specimens in Surveillance Capsule OCI-E

Material description	No. of specimens	
	Tensile	Charpy
Weld metal, WF-112	4	3
Heat-affected zone (HAZ)		
Heat A — C3265-1 (longitud.)	0	8
Baseline material		
Heat A — C3265-1 (longitud.)	4	8
Heat A — C3265-1 (transverse)	0	4
Correlation HSST plate 02	0	8
Total per capsule	8	36

Table 3-3. Chemistry and Heat Treatment of Correlation Material — Heat A-1195-1, A533 Grade B, Class 1 (HSST Plate 02)

Chemical Analysis (1/4T)[a]

Element	Wt %
C	0.23
Mn	1.39
P	0.013
S	0.013
Si	0.21
Ni	0.64
Mo	0.50
Cu	0.17

Heat Treatment

1. Normalized at 1675F ± 75F.
2. 1600F ± 75F for 4 h/water-quenched.
3. 1225F ± 25F for 4 h/furnace-cooled.
4. 1125F ± 25F for 40 h/furnace-cooled.

[a] ORNL-4463.

Table 3-2. Chemistry and Heat Treatment of Surveillance Materials

Chemical Analysis

Element*	Heat C-3265-1	Weld metal WF-112
C	0.21	0.075
Mn	1.42	1.50
P	0.015	0.016
S	0.015	0.006
Si	0.23	0.60
Ni	0.50	0.58
Mo	0.49	0.51
Cu	0.13	0.32

Heat Treatment

Heat No.	Temp, F	Time, h	Cooling
C-3265-1	1600-1650	9.75	Brine quench
	1200-1225	9.5	Brine quench
	1100-1150	40.0	Furnace cooled
WF-112	1100-1150	31.0	Furnace cooled

Figure 3-1. Reactor Vessel Cross Section Showing Surveillance Capsule Locations

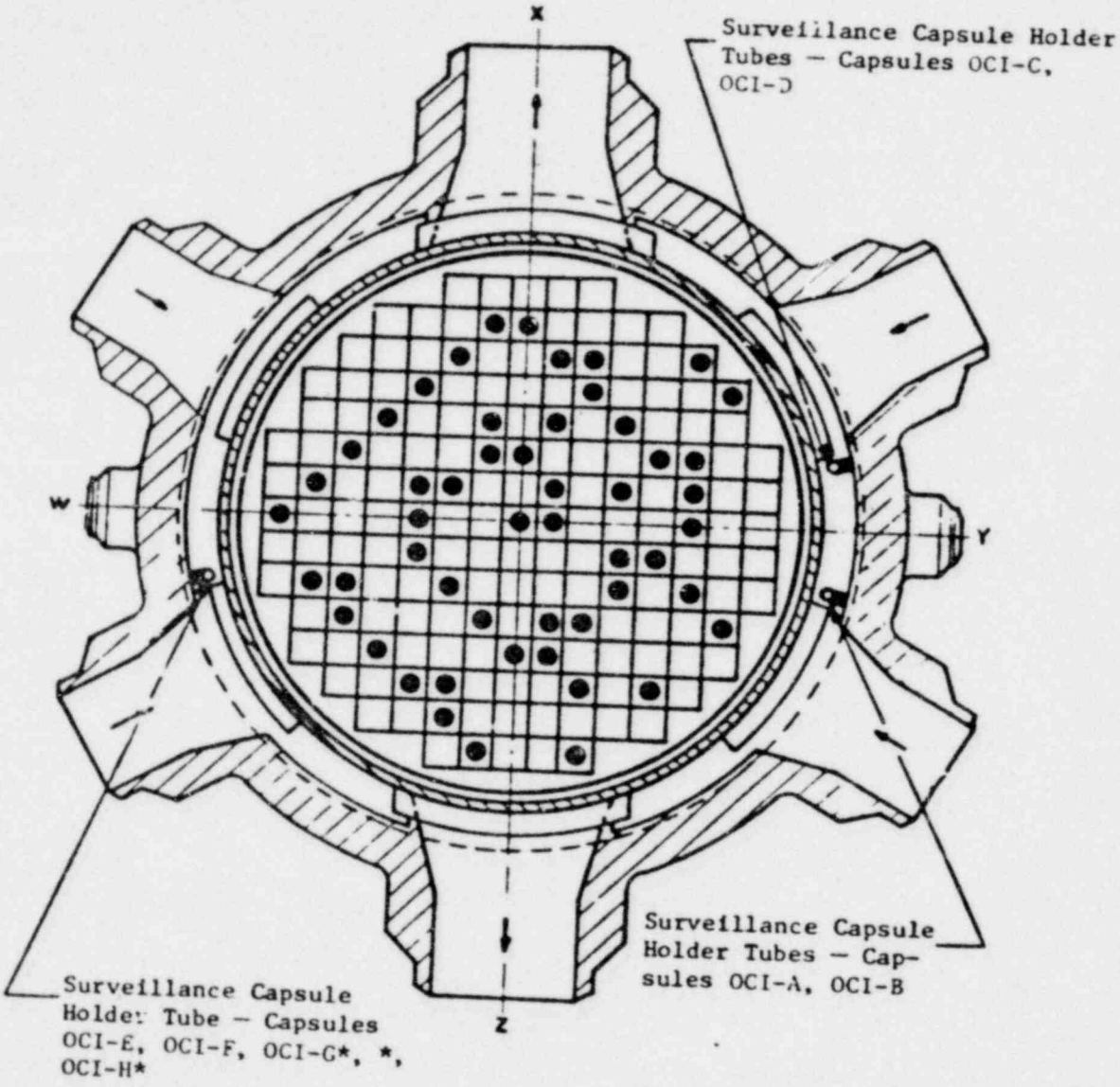

*Thermal aging capsules.

4. PREIRRADIATION TESTS

Unirradiated material was evaluated for two purposes: (1) to establish a baseline of data to which irradiated properties data could be referenced, and (2) to determine those materials properties to the extent practical from available material, as required for compliance with Appendixes G and H to 10 CFR 50.

4.1. Tensile Tests

Tensile specimens were fabricated from the reactor vessel shell course plate and weld metal. The subsize specimens were 4.25 inches long with a reduced section 1.750 inches long by 0.357 inch in diameter. They were tested on a 20,000-lb-load capacity universal test machine at a crosshead speed of 0.005 inch per minute. Test conditions were in accordance with the applicable requirements of ASTM A370-72. For each material type and/or condition, six specimens in groups of three were tested at both room temperature and 600F. An LVDT-type clamp-end screw-on extensometer was used to determine the 0.2% yield point. The tension-compression load cell used had a certified accuracy of better than ± 0.5% of full scale (10,000 lb). All test data for the preirradiation tensile specimens are given in Appendix B.

4.2. Impact Tests

Charpy V-notch impact tests were conducted in accordance with the requirements of ASTM Standard Methods A370-72 and E23-72 on a remote controlled impact tester certified to meet Watertown standards. Test specimens were of the Charpy V-notch type, which are 0.394 inch square and 2.165 inches long.

Prior to testing, specimens were temperature-conditioned in a combination resistance-heated/carbon dioxide-cooled chamber, designed to cover the temperature range from -85 to +550F. The specimen support arm, which is linked to the pneumatic transfer mechanism, is instrumented with a contacting thermocouple allowing instantaneous specimen temperature determinations. Specimens were transferred from the conditioning chamber to the test frame anvil and precisely pretest-positioned with a fully automated, remotely controlled apparatus.

Transfer times were less than 3 seconds and repeat within 0.1 second. Once the specimen was positioned, the electronic interlock opened, and the pendulum was released from its preset drop height. After failing, the specimen, the hammer pendulum was slowed on its return stroke and raised back to its start position. Impact test data for the unirradiated baseline reference materials are presented in Appendix C. Tables C-1 through C-5 contain the basis data which are plotted in Figures C-1 through C-5.

5. POSTIRRADIATION TESTS

5.1. Thermal Monitors

Surveillance capsule OC1-E contained three temperature monitor holder tubes, each containing five fusible alloys with different melting points ranging from 558 to 621F. All the thermal monitors at 558, 580, and 588F had melted, while those at 610 and 621F remained in their original configuration as initially placed in the capsule. From these data it was concluded that the irradiated specimens had been exposed to a maximum temperature in the range of 588 to less than 610F during the reactor vessel operating period. There appeared to be no significant temperature gradient along the capsule length.

5.2. Chemical Analysis

The unirradiated base metal (Heat 3265-1) and the weld metal (WF-112) were analyzed for nickel, copper, phosphorus and sulfur contents to verify original mill test report data. The results from chemical analyses are reported in Table 5-1.

5.3. Tensile Test Results

The results of the postirradiation tensile tests are presented in Table 5-2. Tests were performed on specimens at both room temperature and 580F using the same test procedures and techniques used to test the unirradiated specimens (section 4.1). In general, the ultimate yield strength of the material increased slightly with a corresponding slight decrease in ductility; both effects were the result of neutron radiation damage. The type of behavior observed and the degree to which the material properties changed is within the range of changes to be expected for the radiation environment to which the specimens were exposed.

The results of the preirradiation tensile tests are presented in Appendix B.

5.4. Charpy V-Notch Impact Test Results

The test results from the irradiated Charpy V-notch specimens of the reactor vessel beltline material and the correlation monitor material are presented in Tables 5-3 and 5-4 and Figures 5-1 through 5-5. The test procedures and techniques were the same as those used to test the unirradiated specimens (section 4.2). The data show that the material exhibited a sensitivity to irradiation within the values predicted from its chemical composition and the fluence to which it was exposed.

The results of the preirradiation Charpy V-notch impact test are given in Appendix C.

Table 5-1. Chemistry Data on Unirradiated Oconee 1 RVSP Material

Material type/ heat No.	Composition, wt %			
	Ni	Cu	P	S
Base metal/C-3265-1	0.50	0.17	0.007	0.027
Weld metal/WF-112	0.59	0.32	0.016	0.016

Table 5-2. Tensile Properties of Capsule OCI-E Base Metal and Weld Metal Irradiated to 1.5×10^{18} nvt

Specimen ID No.	Test temp, F	Strength, psi Yield (YS)	Ult. (UTS)	Elongation, % Uniform (UE)	Total (TE)[a]	Red'n of area, %
Base Metal — Heat C-3265-1, Longitudinal						
AAE 704	RT	67,430	89,510	10.97	22.06	68.3
AAE 721	RT	67,430	87,910	10.51	21.60	69.8
Mean, $\bar{x}$		67,430	88,710	10.74	21.83	69.04
Std dev'n, 6		0	800	0.23	0.23	0.75
AAE 708	580	61,440	88,810	13.35	26.13	67.4
AAE 730	580	61,440	89,910	10.84	21.40	69.8
Mean, $\bar{x}$		61,440	89,360	12.35	23.77	68.6
Std dev'n, 6		0	550	1.505	2.365	1.2
Weld Metal — WF-112						
AAE 109	RT	77,920	93,910	12.82	24.66	56.3
AAE 120	RT	79,920	95,710	12.32	23.04	57.1
Mean, $\bar{x}$		78,920	94,810	12.57	23.85	56.7
Std dev'n, 6		1,000	900	0.25	0.81	0.4
AAE 110	580	69,930	91,860	10.12	16.2	44.1
AAE 126	580	69,930	92,410	9.49	15.73	45.7
Mean, $\bar{x}$		69,930	92,135	9.81	15.97	44.9
Std dev'n, 6		0	275	0.315	0.235	0.8

[a] TE values calculated from chart record.

Table 5-3. Charpy Impact Data for Capsule OCI-E Base Metal Irradiated to 1.5×10^{18} nvt

Specimen ID No.	Test temp, F	Abs energy, ft-lb	Lateral expans, 10^3 in.	Shear fracture, %
Heat C-3265-1, Longitudinal				
AAE 708	325	139	77.5	100
730	201	131.5	66	100
721	120	110	70.5	55
746	106	92	65	35
709	92	72	57	18
723	73	52	41	8
706	70	66	52	15
753	63	44	36	4
Heat C-3265-1, Transverse				
AAE 611	203	107	69	100
610	147	74	56	75
630	97	50	40	12
613	79	44	37.5	8
HAZ — Heat C-3265-1, Longitudinal				
AAE 403	318	86	67	100
423	199	83	54.5	100
439	120	65	54	92
436	100	74	54	85
418	63	70	45	75
452	27	67	46	25
435	13	39	29	20
420	-21	36	26	10

Table 5-4. Charpy Impact Data for Capsule OCI-E Weld Metal (WF-112) Irradiated to 1.5×10^{18} nvt

Specimen ID No.	Test temp, F	Abs energy, ft-lb	Lateral expans, 10^3 in.	Shear fracture, %
AAE 059	315	55	49.5	100
037	198	52.5	45.5	96
003	170	36	35.5	55
041	170	44	34	50
044	152	52	49.5	85
048	121	42	30	35
058	89	33	29.5	12
056	62	27	22.5	8

Table 5-5. Charpy Impact Data for Capsule OCI-E Correlation Monitor Material Irradiated to 1.5×10^{18} nvt

Specimen ID No.	Test temp, F	Abs energy, ft-lb	Lateral expans, 10^3 in.	Shear fracture, %
AAE 929	428	104	73.5	100
935	321	111	71	100
966	260	98	69	95
964	197	78	52	65
908	154	57	42.5	30
927	120	50	39	30
971	99	36	30	6
967	62	28	22.5	2

Figure 5-1. Charpy Impact Data From Irradiated Base Metal, Longitudinal Orientation

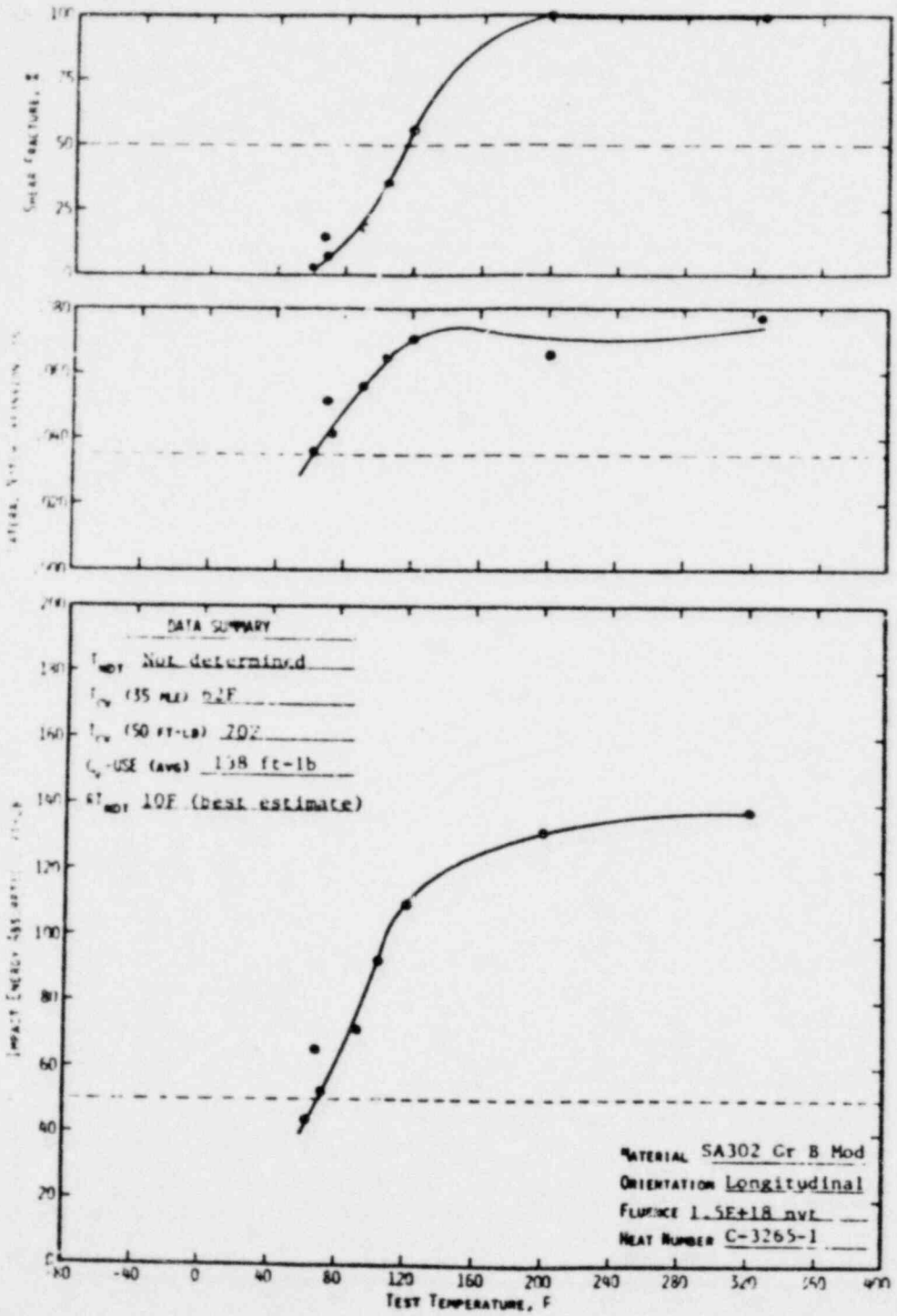

Figure 5-2. Charpy Impact Data From Irradiated Base Metal, Transverse Orientation

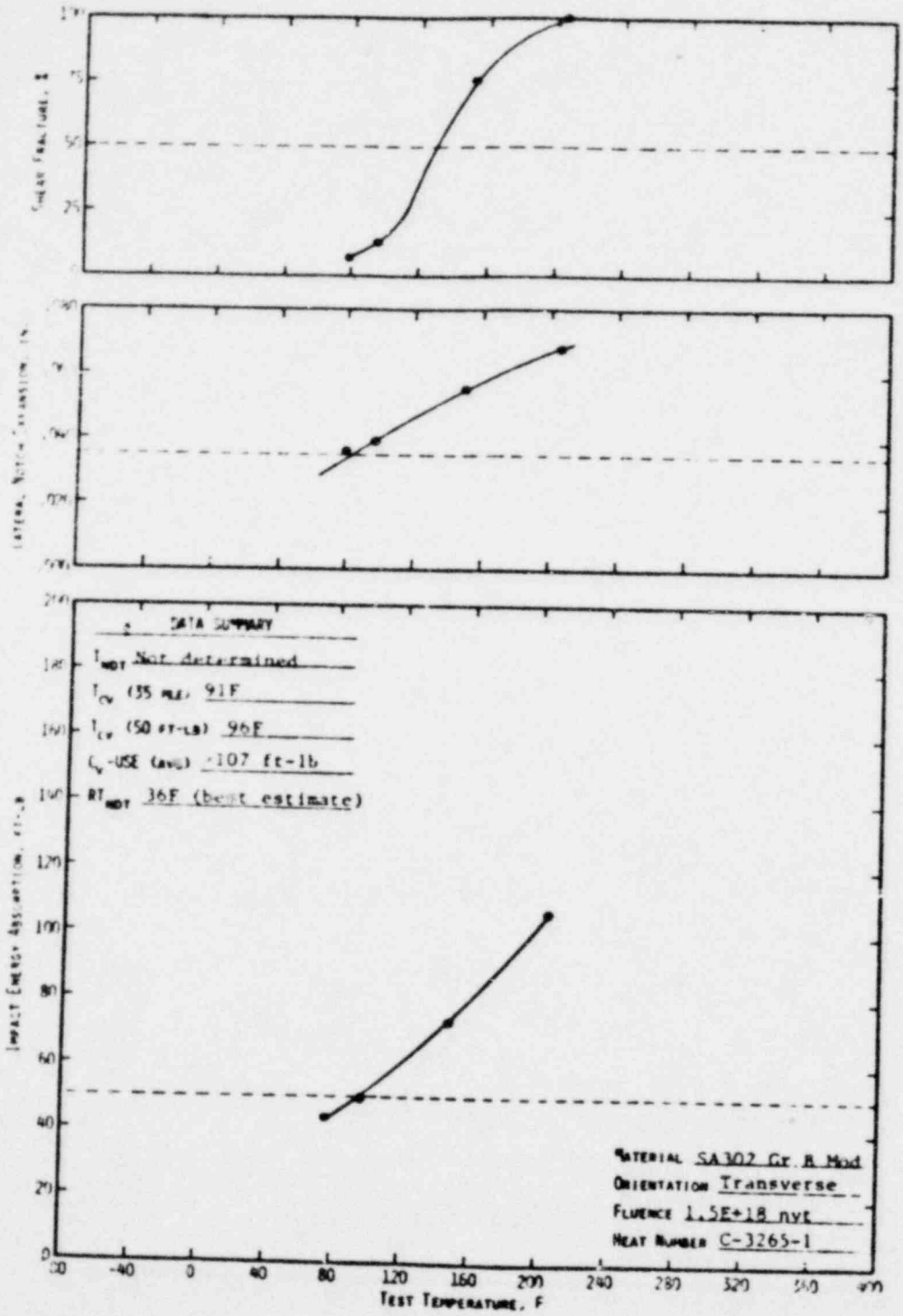

Figure 5-3. Charpy Impact Data From Irradiated Base Metal Heat-Affected Zone, Longitudinal Orientation

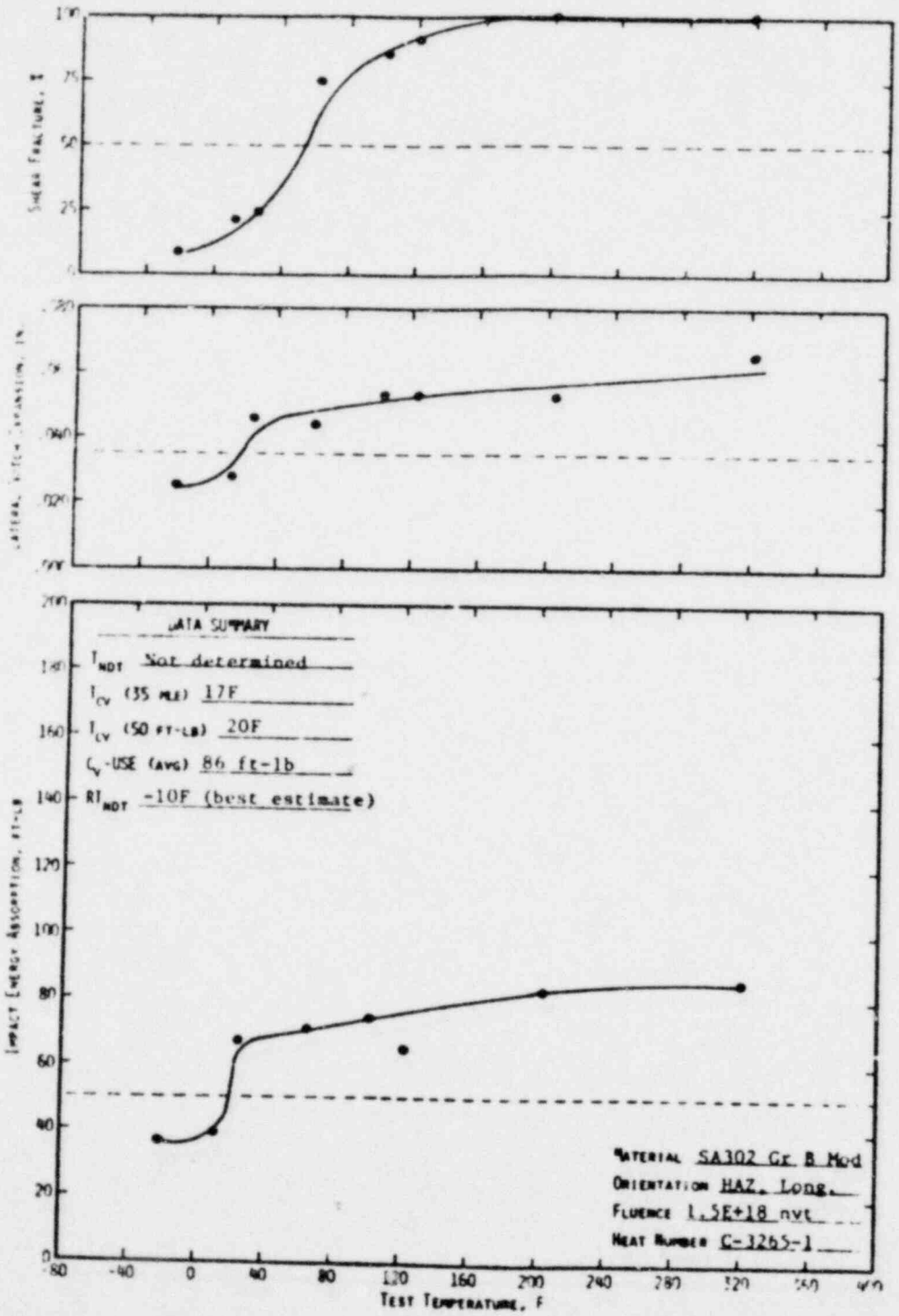

Figure 5-4. Charpy Impact Data From Irradiated Weld Metal

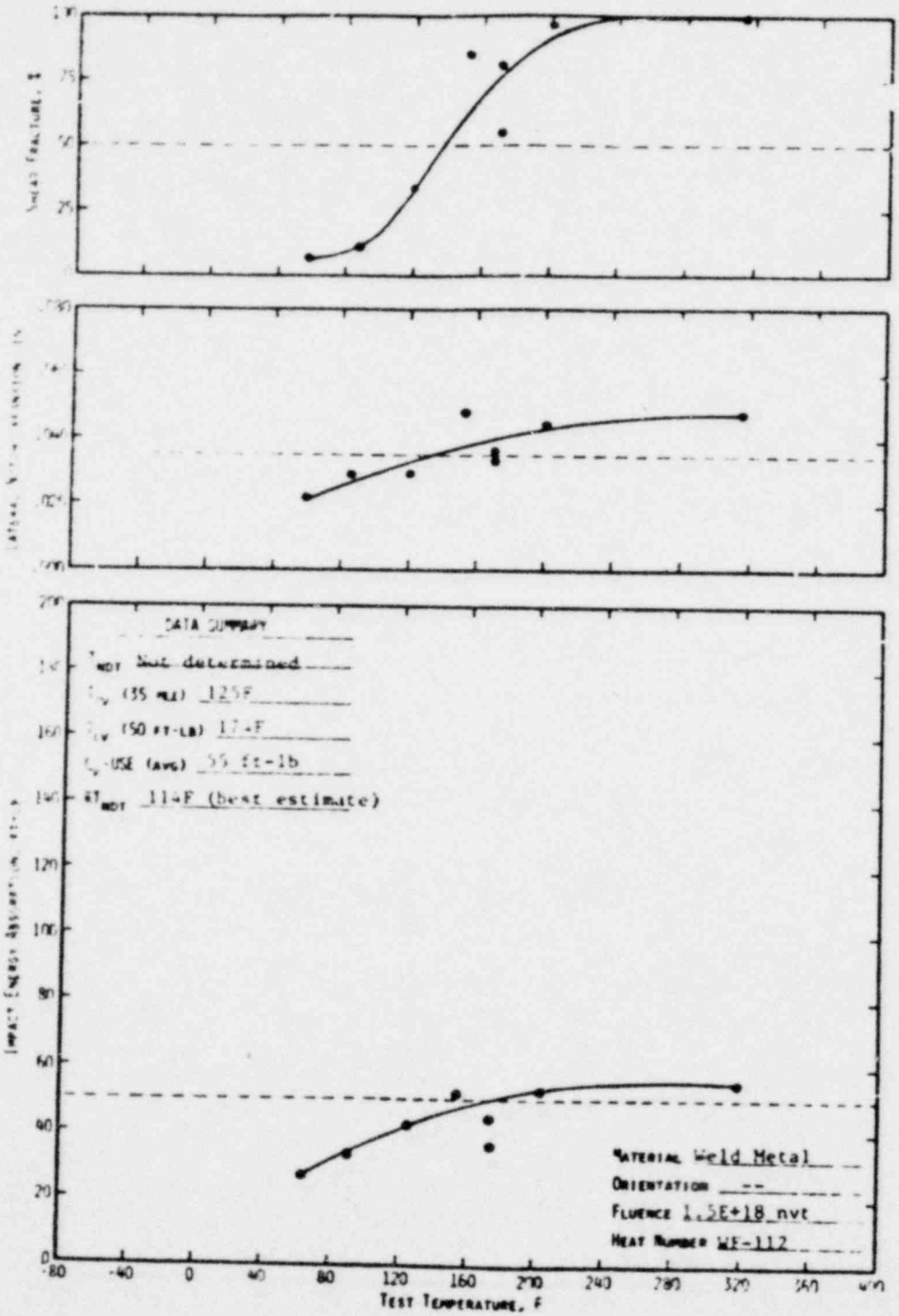

Figure 5-5. Charpy Impact Data From Irradiated Correlation Monitor Material

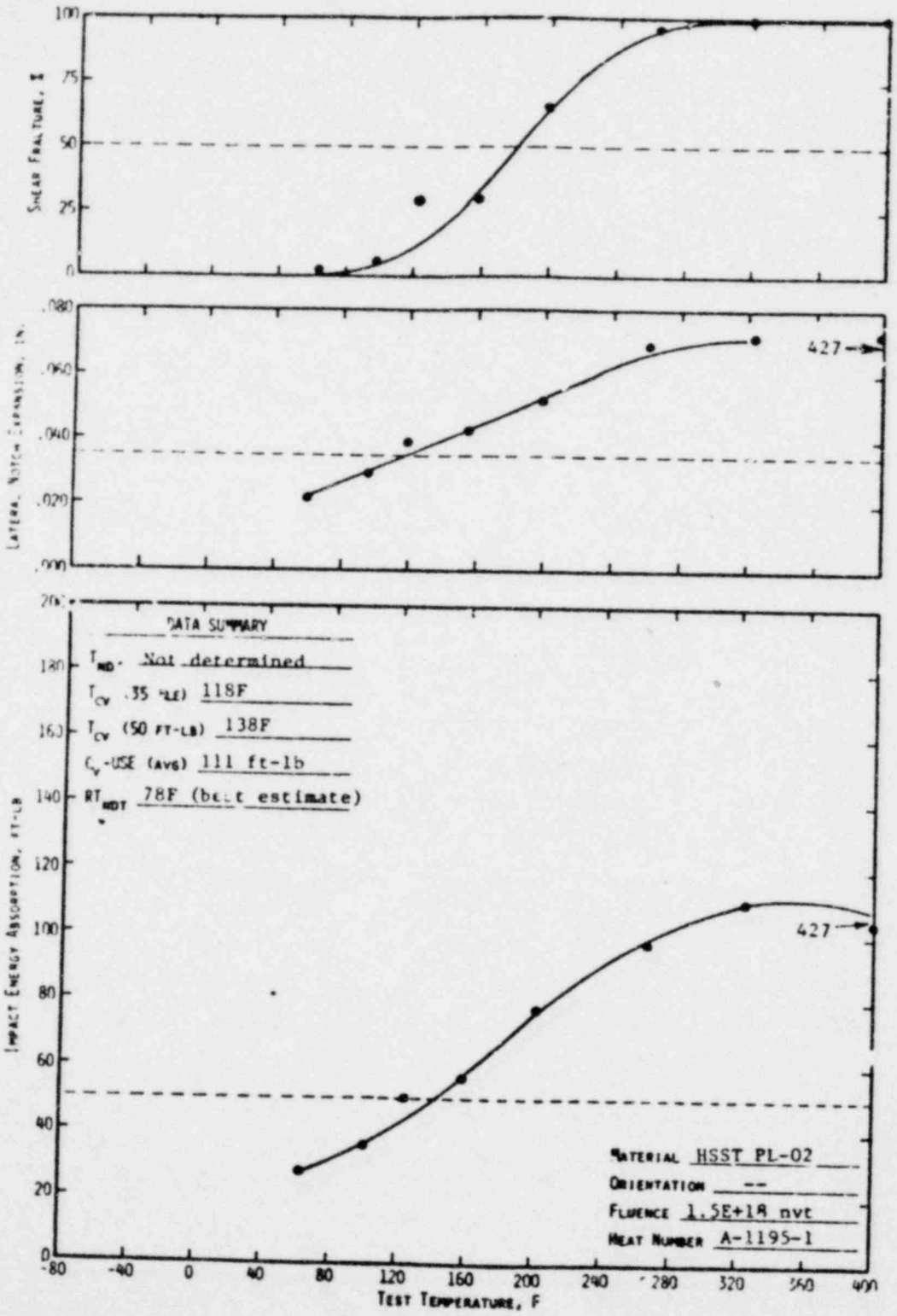

6. NEUTRON DOSIMETRY

6.1. Introduction

A significant aspect of the surveillance program is to provide a correlation between the neutron fluence above 1 MeV and the radiation-induced property changes noted in the surveillance specimen. To permit such a correlation, activation detectors with reaction thresholds in the energy range of interest were placed in each surveillance capsule. The properties of interest for the detectors are given in Table 6-1.

Because of a long half life of 30 years and an effective energy range of 0.5 MeV or greater, only the measurements of ^{137}Cs production from fission reactions in ^{237}Np (and possibly ^{238}U) are directly applicable to analytical determinations of fast neutron (E > 1 MeV) fluence over cycles 1 and 2. The other dosimeters are useful as corroborating data for shorter time intervals and/or higher energy fluxes. Comparisons of measured data (cycles 1 and 2) to calculated results require the use of calculated data previously reported for cycle 1 to augment the cycle 2 analysis presented here.

The energy-dependent neutron flux is not directly available from the activation detectors because the process provides the integrated effect of the neutron flux on the target material as a function of both irradiation time and neutron energy. To obtain an accurate estimate of the average neutron flux incident upon the detector, the following parameters must be known: (1) the operating history of the reactor, (2) the energy response of the given detector, and (3) the neutron spectrum at the detector location. Of these parameters the definition of the neutron spectrum is the most difficult to obtain. Essentially, the two means available for obtaining the spectrum are iterative unfolding of experimental foil data and analytical methods. Due to a lack of sufficient threshold foil detectors satisfying both the threshold energy and the half-life requirements necessary for a surveillance program, iterative unfolding could not be used; this leaves the specification of the neutron spectrum to the analytical method.

6.2. Analytical Approach

Energy-dependent neutron fluxes seen by the detector were determined by a discrete ordinate solution of the Boltzmann transport equation. Specifically, ANISN[3], a one-dimensional code, and DOT[4], a two-dimensional code, were used to calculate the flux at the detector position. In both codes the Oconee system was radially modeled from the core out to the air gap outside the pressure vessel. The model included the core with a time-averaged radial power distribution, core liner, barrel, thermal shield, pressure vessel, and water regions. Including the internal components enables the analytical method to account for the distortions of the required energy spectrum by attenuation in these components. The ANISN code used the CASK[5], 22-group neutron cross sectional set with an S_6 order of angular quadrature and a P_3 expansion of the scattering matrix. The problem was run along a radius across the core flats. Azimuthal variations were obtained with a DOT r-theta calculation that modeled one-eighth of a plan view of the core and included a pin-by-pin, time-averaged power distribution. The DOT calculation used S_6 quadrature and a P_1 cross section set derived from CASK.

Fluxes calculated with this DOT model must be adjusted to account for the lack of P_3 cross-sectional detail in calculations of anisotropic scattering, a perturbation caused by the presence of the capsule, and the axial power distribution. The first two items are both energy- and position-dependent. A P_3/P_1 correction factor was obtained by comparing two ANISN 1-D model calculations in which only the order of scattering was varied. The capsule perturbation factor was obtained from a comparison of two DOT x-y model calculations — one with a capsule explicitly modeled with SS304 cladding, Al filler region, and carbon steel specimens and the other with water in those regions. The effect of axial power distribution was determined from a previous DOT r-z model using an estimated average (axial) over three fuel cycles. The net results from these parameter studies was a flux adjustment factor K (Table 6-2), which should be applicable to the appropriate dosimeters in all 177-FA surveillance programs in which the capsules are located at a radius of 211 centimeters from the core center and at 11° from a major axis.

The calculation described above provides the neutron flux as a function of energy at the detector position. These calculated data are used in the following equations to obtain the calculated activities used for comparison with the experimental values. The basic equation[6] for the activity D (in μCi/g) is

$$D_i = \frac{CN}{A_i \; 3.7 \times 10^{-4}} f_i \sum_E \sigma_n(E)\phi(E) \sum_{j=1}^{M} F_j(1-e^{-\lambda_i t_j})e^{-\lambda_i(T-\tau_j)} \qquad (6\text{-}1)$$

where

C = normalizing constant (ratio of measured to calculated flux),

N = Avagadro's number,

A_n = atomic weight of target material n,

f_i = either weight fraction of target isotope in nth material or fission yield of desired isotope,

$\sigma_n(E)$ = group-averaged cross sections for material n (listed in Table D-4),

$\phi(E)$ = group-averaged fluxes calculated by DOT analysis,

F_j = fraction of full power during jth time interval t_j,

λ_i = decay constant of ith material,

t_j = interval of power history,

T = sum of total irradiation time, i.e., residual time in reactor and wait time between reactor shutdown and counting,

τ_j = cumulative time from reactor startup to end of jth time period, i.e.,

$$\tau_j = \sum_{k=1}^{j} t_k.$$

The normalizing constant C can be obtained by equating the right side of equation 6-1 to the measured activity. With C specified the neutron fluence greater than 1 MeV can be calculated from

$$\phi(E > 1.0 \text{ MeV}) = C \sum_{E=1}^{15 \text{ MeV}} \phi(E) \sum_{j=1}^{M} F_j t_j \qquad (6\text{-}2)$$

where M is the number of irradiation time intervals; the other values are defined above.

6.3. Results

Calculated activities are compared to measurements of the dosimeters in Table 6-3. The ^{137}Cs data show that fast flux (E > 1 MeV) is somewhat underpredicted (~10%) by the analytical model described (if one assumes that the calculated flux spectrum is correct). Such an agreement is probably within the uncertainty limits of this analysis. However, for conservatism a flux normalization factor of 1.1 is recommended for fast neutron calculations near the pressure

vessel. The ^{103}Ru activities (because of a short half-life) are indicative of the validity of the analytical model representation of the latter part of cycle 2. ^{54}Mn and ^{57}Co activities show an overprediction (~25%) of 2 MeV or greater flux by the analytical model. The significance of these results to the fast flux calculation is somewhat lessened since approximately 40% of the neutrons with E greater than 1 MeV are in the 1 to 2 MeV range (Table 6-4). The possibility exists that an inherent overprediction of flux occurs in the analytical model and that measurements of activities from fission wires are high. It is also possible that the core leakage flux over the latter part of cycle 2 was less than the average for all of cycle 2; this could account for C being less than one since calculated data are based on an average leakage flux and measured data for short-lived isotopes are based on the latter part of the cycle. Future surveillance capsule data should clarify this supposition.

The agreement between C values for long-lived and short-lived dosimeters indicates that the fission dosimeter normalization constant reported in reference 2 is in error and lends credence to the suggested occurrence of incorrect activity measurements after cycle 1. Therefore, cycle 1 fast fluxes have been recalculated with a 1.1 normalizing constant and are presented with cycle 2 data in Table 6-5. Average fast flux over cycles 1 and 2 was extrapolated to a 40-year lifetime with a 0.8 use factor to obtain fluence at the pressure vessel wall of 1.7×10^{19} n/cm^2 (2568 MWt); this can be compared to a predicted value of 2.9×10^{19} n/cm^2 (based on an estimated power distribution over three cycles) reported in reference 7 for a reactor at 2772 MWt. An average lead factor of 1.7 differs from a predicted value[9] of 1.4 primarily because of flux pertubation due to the presence of the capsule (a factor not previously considered).

An extension of the flux range down to 0.1 MeV was calculated based on the same normalization factor (1.1) being applicable. Since no dosimeter reactions cover that range, additional uncertainty is introduced into the results. The data, which are included in Table 6-5, indicate that fluences are essentially doubled when the energy range is extended from 1 to 0.1 MeV.

Table 6-1. Surveillance Capsule Detectors

Detector reaction	Threshold energy, MeV	Isotope half-life
$^{54}Fe(n,p)^{54}Mn$	2.0	303 days
$^{58}Ni(n,p)^{58}Co$	2.5	71.3 days
$^{238}U(n,f)^{137}Cs$	1.5	30 years
$^{237}Np(n,f)^{137}Cs$	0.5	30 years
$^{238}U(n,f)^{103}Ru$	1.5	39.5 days
$^{237}Np(n,f)^{103}Ru$	0.5	39.5 days

Table 6-2. Flux Adjustment Factor

Energy range, MeV	Axial power factor	P_3/P_1	Capsule perturb'n	γ
>0.1	1.1	1.22	1.40	1.88
>1	1.1	1.23	1.20	1.62
>2	1.1	1.24	1.04	1.42
>2.5	1.1	1.25	0.96	1.32

Table 6-3. Dosimeter Activations After Cycle 2

Reaction	A measured activity,[a] μCi/g	B — Calculated activity[b], μCi/g: Cycle 2	Cycle 1	cycles 1 and 2 decayed[c]	C = A/B normalization constant
$^{54}Fe(n,p)^{54}Mn$	536.5	595.9	397	729.3	0.74
$^{58}Ni(n,p)^{58}Co$	975.3	1295.5	685	1266	0.77
$^{238}U(n,f)^{137}Cs$	1.943	1.100	0.638	1.719	1.13
$^{237}Np(n,f)^{137}Cs$	9.32	5.709	3.19	8.799	1.06
$^{238}U(n,f)^{103}Ru$	52.65	53.18	23.4	53.19	0.99
$^{237}Np(n,f)^{103}Ru$	254.3	246.6	106	246.6	1.03

(a) Average of four dosimeter wires from Table D-3.

(b) Values from reference 2 were multiplied by 1.1 to account for axial power distribution (not included). ^{54}Mn and ^{58}Co values were converted to gram of target (reference 1 values were per gram of dosimeter).

(c) Cycle 1 values were decayed over the time interval from the end of cycle 1 to the end of cycle 2 and then added to cycle 2.

$$D_{1,2} = D_2 + D_1 e^{-\lambda_i t}$$

Table 6-4. Normalized Flux Spectra, E > 1 MeV

Energy range, MeV	In water near pressure vessel wall	^{235}U fission
12.2 - 15.0	0.0015	0.0002
10.0 - 12.2	0.0063	0.0013
8.18 - 10.0	0.0181	0.0052
6.36 - 8.18	0.0499	0.021
4.96 - 6.36	0.0906	0.051
4.06 - 4.96	0.0784	0.052
3.01 - 4.06	0.1159	0.159
2.46 - 3.01	0.1200	0.132
2.35 - 2.46	0.0389	0.034
1.83 - 2.35	0.1506	0.178
1.11 - 1.83	0.2832	0.323
1.0 - 1.11	0.0466	0.044
Total	1.000	1.000

Table 6-5. Fast Neutron Fluence

	Cycle 1 309.3 days	Cycle 2 291.2 days	Cycles 1 and 2 600.5 days	Lifetime 32 years[a]
Capsule Center				
Fast flux (E > 1 MeV)	2.13 + 10	3.76 + 10	--	--
Nvt (E > 1 MeV)	5.7 + 17	9.5 + 17	1.5 + 18	2.9 + 19
Flux (E > 0.1 MeV)	4.27 + 10	7.53 + 10		
Nvt (E > 0.1 MeV)	1.1 + 18	1.9 + 18	3.0 + 18	5.9 + 19
Pressure Vessel Wall				
Fast Flux (E > 1 MEV)	1.37 + 10	2.08 + 10	--	--
Nvt (E > 1 MeV)	3.7 + 17	5.2 + 17	8.9 + 17	1.7 + 19
Flux (E > 0.1 MeV)	2.78 + 10	4.22 + 10		
Nvt (E > 0.1 MeV)	7.4 +17	1.1 + 18	1.8 + 18	3.5 + 19

[a] Extrapolation of average flux in cycles 1 and 2.

Table 6-6. Predicted Fast Fluence in Pressure Vessel for 10 EFPY[a]

	Inside wall	T/4	3 T/4	Outside wall
Average fast flux, n/cm^2-s	1.8 + 10	1.0 + 10	2.4 + 9	1.0 + 9
Fast fluence n/cm^2	5.7 + 18	3.2 + 18	7.6 + 7	3.2 + 17

[a] These data are based on the hypothesis that pressure vessel fluence is proportional to calculated average core leakage fluxes for cycles 3 and 4 combined with specimen analyses for cycles 1 and 2. Subsequent fuel cycles were assumed to be the same as cycle 4.

Figure 6-1. Predicted Fast Neutron Fluences at Various Locations Through Reactor Vessel Wall for First 10 EFPY (Oconee 1)

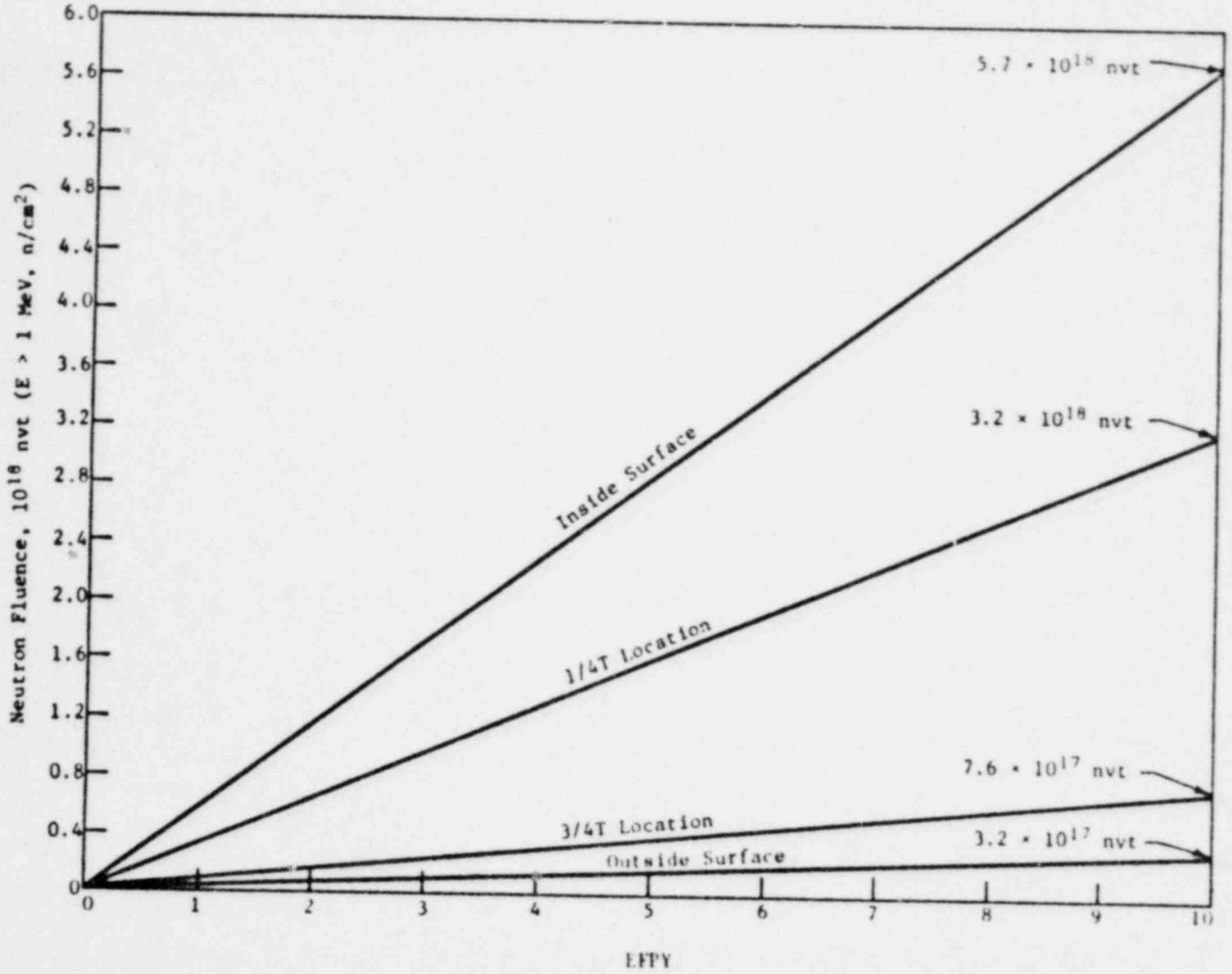

7. DISCUSSION OF CAPSULE RESULTS

7.1. Preirradiation Property Data

A review of the unirradiated properties of the reactor vessel core belt region indicated no significant deviation from expected properties except in the case of the upper shelf properties of the weld metal. Based on the predicted end-of-service peak neutron fluence value at the 1/4T vessel wall location and the copper content of this weld, it is predicted that the end-of-service Charpy upper shelf energy (USE) will be below 50 ft-lb. This weld was selected for inclusion in the surveillance program in accordance with the criteria in effect at the time the program was designed for Oconee 1. The applicable selection criterion was based on the unirradiated properties only.

7.2. Irradiated Property Data

7.2.1. Tensile Properties

Table 7-1 compares irradiated and unirradiated tensile properties. At both room temperature and elevated temperature, the ultimate and yield strength changes in the base metal as a result of irradiation and the corresponding changes in ductility are negligible. There appears to be some strengthening, as indicated by increases in ultimate and yield strength and similar decreases in ductility properties. All changes observed in the base metal are so small as to be considered within experimental error. The changes at both room temperature and 580F in the properties of the weld metal are greater than those observed for the base metal, indicating a greater sensitivity of the weld metal to irradiation damage. In either case, the changes in tensile properties are insignificant relative to the analysis of the reactor vessel materials at this period in service life.

7.2.2. Impact Properties

The behavior of the Charpy V-notch impact data is more significant to the calculation of the reactor system's operating limitations. Table 7-2 compares

the observed changes in irradiated Charpy impact properties with the predicted changes as shown in Figures 7-1 through 7-5.

The 50-ft-lb transition temperature shift for the weld metal and the base metal was in good agreement with the shift that would be predicted according to Regulatory Guide 1.99. A similar comparison of the shift of the correlation monitor material shows good agreement. The less-than-ideal comparison may be attributed to the spread in the data of the unirradiated material combined with a minimum of data points to establish the irradiated curve. Under these conditions, the comparison indicates that the estimating curves in RG 1.99 for medium-copper materials and at medium fluence levels are reasonably accurate for predicting the 50-ft-lb transition temperature shifts. The estimating curves for high-copper material at medium fluence levels are also in good agreement with the observed data.

The increase in the 35-mil lateral expansion transition temperature is compared with the shift in RT_{NDT} curve data in a manner similar to the comparison made for the 50-ft-lb transition temperature shift. These data show a behavior similar to that observed from the comparison of the observed and predicted 50-ft-lb transition data.

The data for the decrease in Charpy USE with irradiation showed a poor agreement with predicted values for both the base matals and the weld metal. However, the weld metal data compares well with the predicted value in view of the lack of data for high-copper-content weldments at low to medium fluence values that were used to develop the estimating curves.

The RT_{NDT} shifts shown are in good agreement with those predicted from Regulatory Guide 1.99 at the fluence level of this capsule. This good agreement is probably attributable to two factors. First, the fluence level is approaching that for which the bulk of the data used to generate the prediction curves was located. Second, the re-analysis of the chemical composition of the irradiated materials gives a more reliable value for comparison of observed versus predicted values.

Results from other capsules indicate that the RT_{NDT} estimating curves have greater inaccuracies at the very low neutron fluence levels ($\leq 1 \times 10^{18}$ n/cm^2). This inaccuracy is attributed to the limited data at the low fluence values and of the fact that the majority of the data used to define the curves in RG 1.99 are based on the shift at 30 ft-lb as compared to the current

requirement of 50 ft-lb. For most materials the shifts measured at 50 ft-lb/35 MLE are expected to be higher than those measured at 30 ft-lb. The significance of the shifts at 50 ft-lb and/or 35 MLE is not well understood at present, especially for materials having USEs that approach the 50 ft-lb level and/or the 35 MLE level. Materials with this characteristic may have to be evaluated at transition energy levels lower than 50 ft-lb.

The design curves for predicting the shift at 50 ft-lb/35 MLE will probably be modified as data become available; until that time, the design curves for predicting the RT_{NDT} shift as given in Regulatory Guide 1.99 are considered adequate for predicting the RT_{NDT} shift of those materials for which data are not available and will continue to be used to establish the pressure-temperature operational limitations for the irradiated portions of the reactor vessel.

The lack of good agreement of the change in Charpy USE is further support of the inaccuracy of the prediction curves at the lower fluence levels. Although the prediction curves are conservative in that they predict a larger drop in upper shelf than is observed for a given fluence and copper content, the conservatism can unduly restrict the operational limitations. These data support the contention that the USE drop curves will have to be modified as more reliable data become available; until that time the design curves used to predict the decrease in USE are conservative.

Table 7-1. Comparison of Tensile Test Results

	Room temp test		Elevated temp test[a]	
	Unirr	Irrad	600F	580F
Base Metal – C-3265-1, Longitudinal				
Fluence, 10^{18} n/cm^2 (> 1 MeV)	0	1.5	0	1.5
Ult. tensile strength, ksi	86.1	88.7	64.4	89.3
0.2% yield strength, ksi	64.3	67.4	58.0	61.4
Elongation, %	26.5	21.8	27.3	23.7
RA, %	68.0	69.0	70.0	68.6
Weld Metal – WF-112				
Fluence, 10^{18} n/cm^2 (> 1 MeV)	0	1.5	0	1.5
Ult. tensile strength, ksi	80.5	94.8	80.8	92.1
0.2% yield strength, ksi	63.3	78.9	56.4	63.9
Elongation, %	30.9	23.8	24.4	15.9
RA, %	63.0	56.7	61.0	44.9

[a] The differences in test temperatures are the result of the unirradiated specimens being tested before removal and evaluation of the capsule thermal monitors.

Table 7-2. Observed Vs Predicted Changes in Irradiated Charpy Impact Properties

Material	Observed	Predicted[a]
Increase in 50-ft-lb trans temp, F		
Base material (C-3265-1)		
Longitudinal	33	46
Transverse	32	48
Heat-affected zone (C-3265-1)	33	48
Weld metal (WF-112)	124	124
Correlation material (A-1195-1)	64	60
Increase in 35-MLE trans temp, F		
Base material (C-3265-1)		
Longitudinal	58	48[b]
Transverse	43	48[b]
Heat-affected zone (C-3265-1)	34	48[b]
Weld metal (WF-112)	109	124[b]
Correlation material (A-1195-1)	63	60[b]
Decrease in Charpy USE, ft-lb		
Base material (C-3265-1)		
Longitudinal	3	24
Transverse	ND	18
Heat-affected zone (C-3265-1)	27	19
Weld metal (WF-112)	9	19
Correlation material (A-1195-1)	19	26

[a] These values predicted per Regulatory Guide 1.99, Revision 1.

[b] Based on the assumption that MLE as well as 50-ft-lb transition temperature is used to control the shift in RT_{NDT}.

ND — Not determined.

Figure 7-1. Irradiated Vs Unirradiated Charpy Impact Properties of Base Metal, Longitudinal Orientation

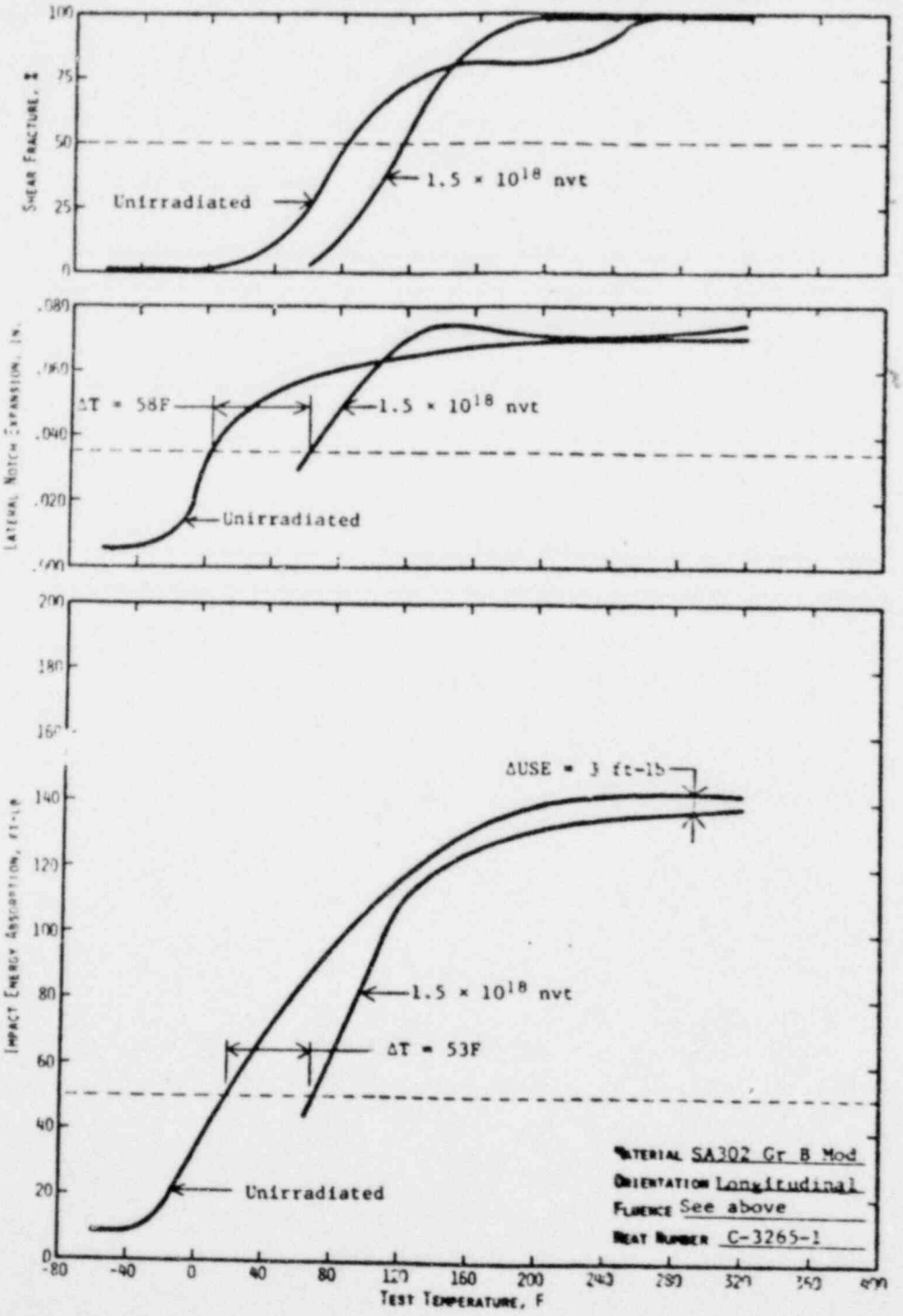

Figure 7-2. Irradiated Vs Unirradiated Charpy Impact Properties of Base Metal, Transverse Orientation

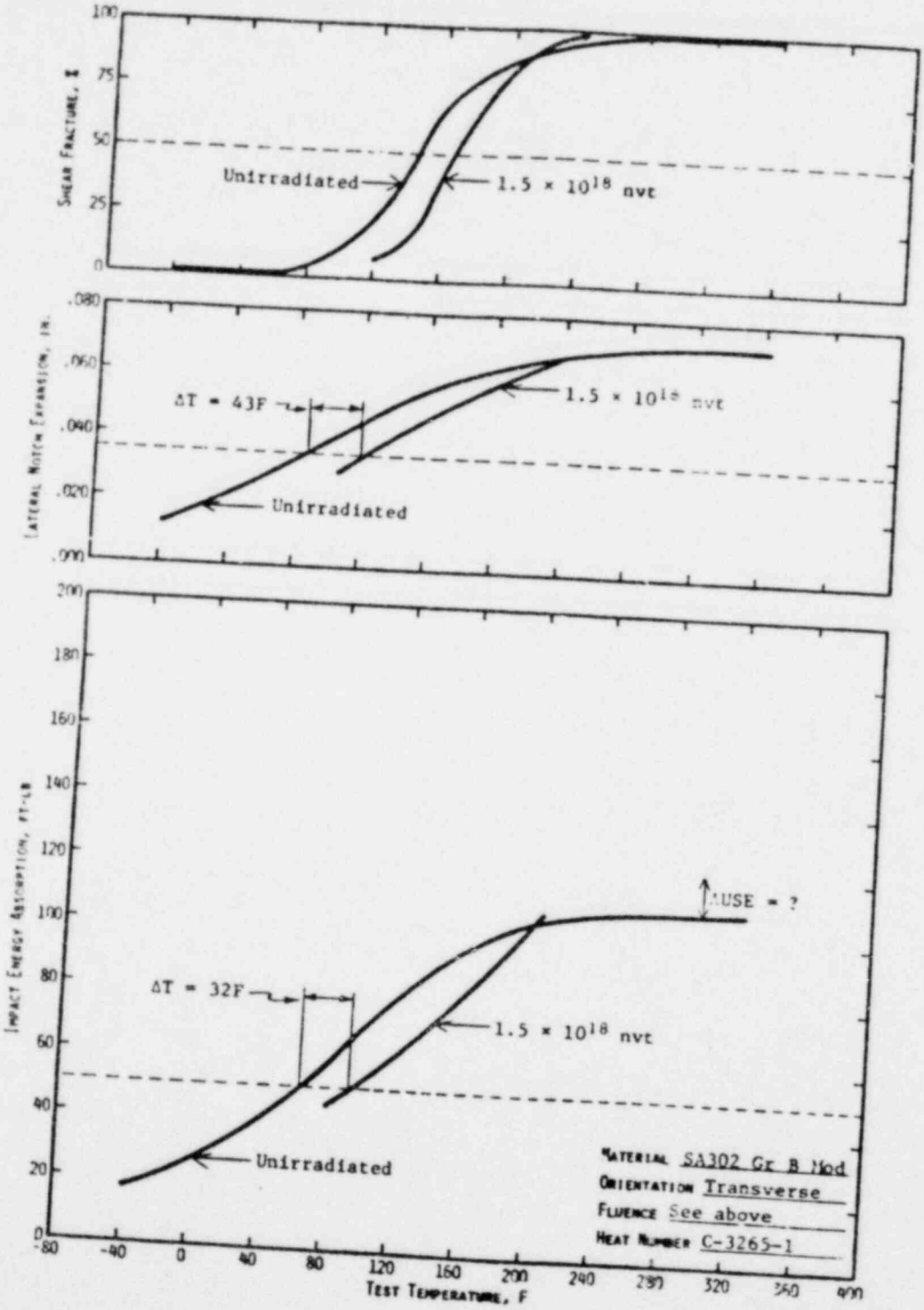

Figure 7-3. Irradiated Vs Unirradiated Charpy Impact Properties of Base Metal, Heat-Affected Zone, Longitudinal Orientation

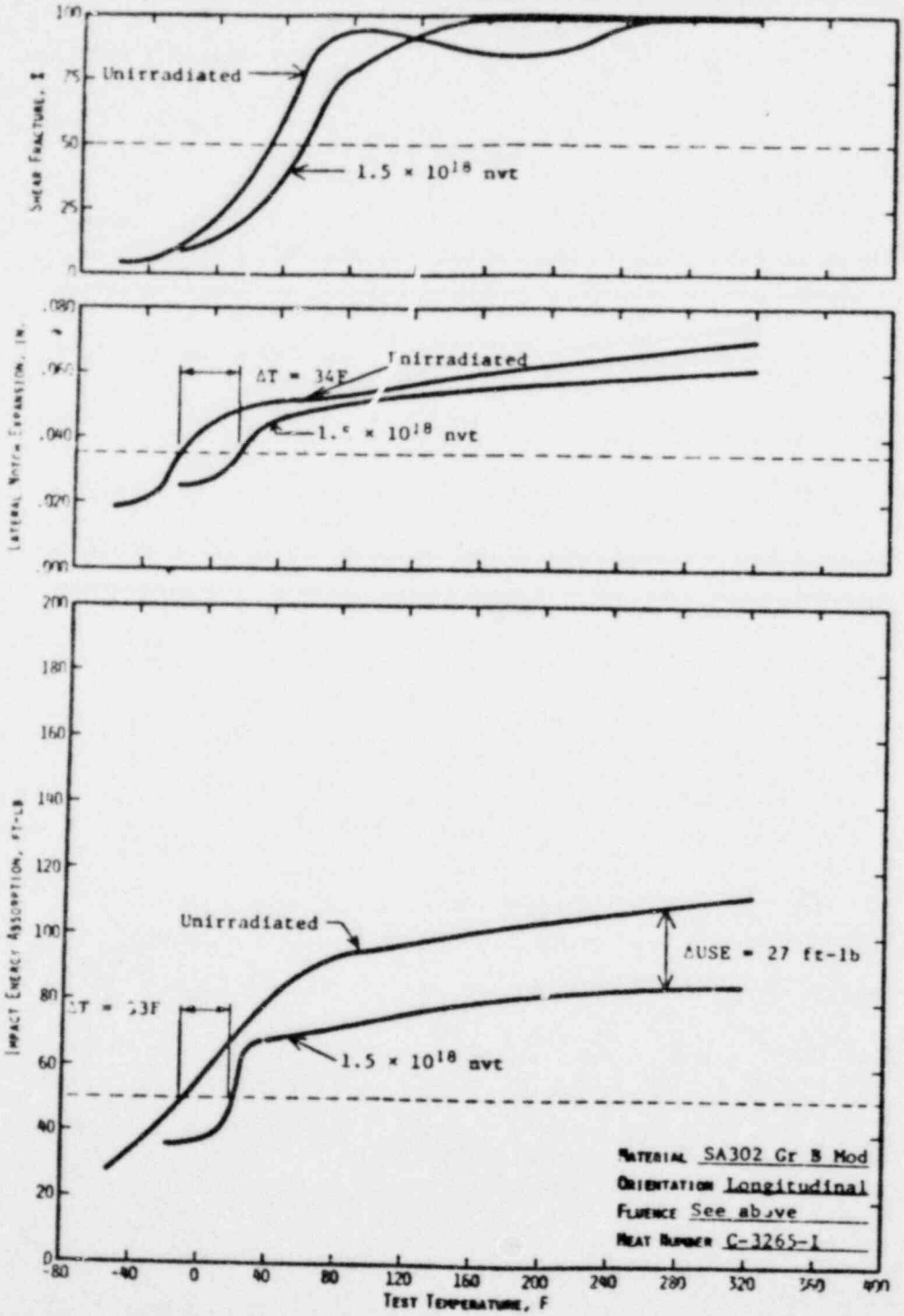

Figure 7-4. Irradiated Vs Unirradiated Charpy Impact Properties of Weld Metal

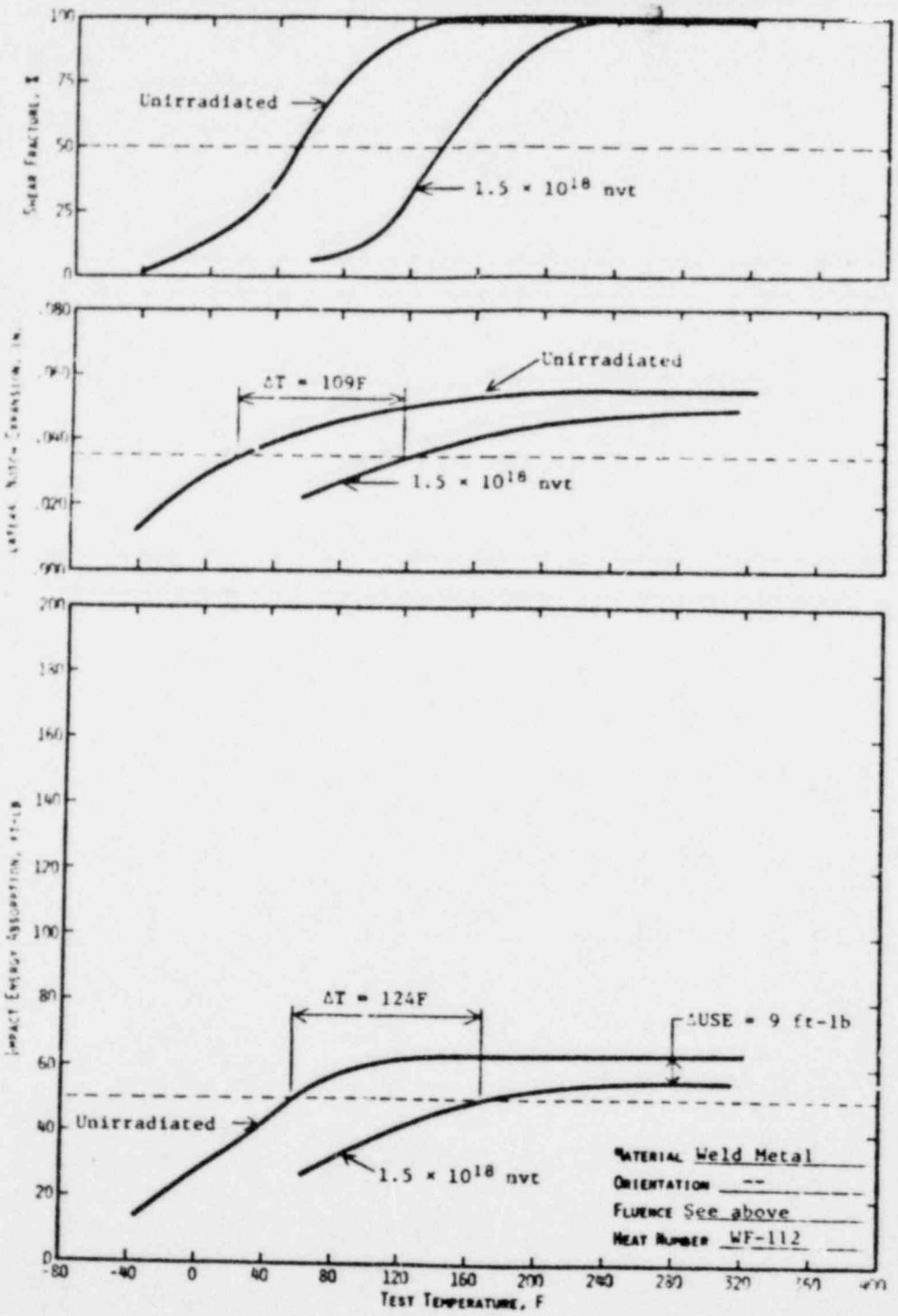

Figure 7-5. Irradiated Vs Unirradiated Charpy Impact Properties of Correlation Monitor Material

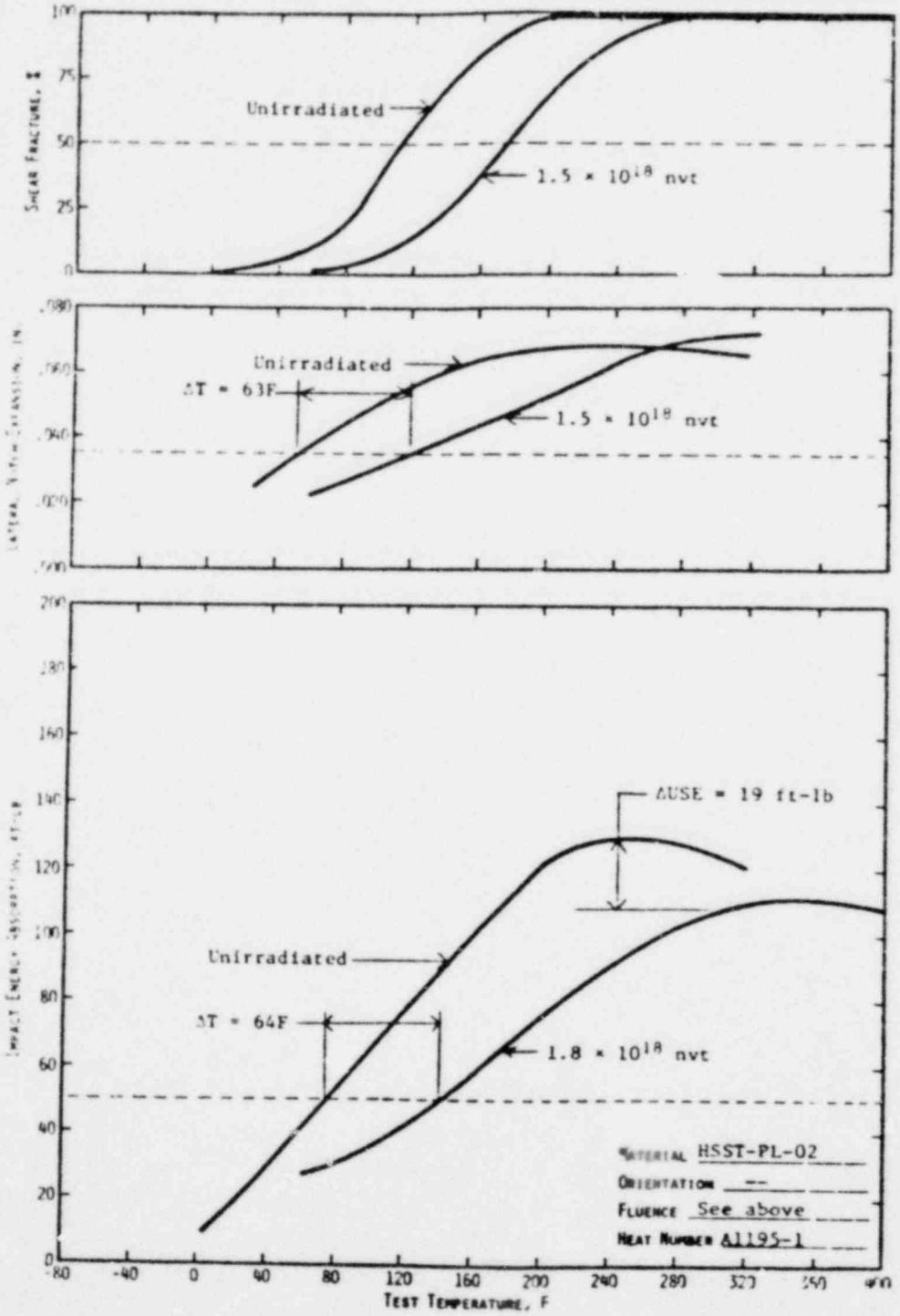

8. DETERMINATION OF RCPB PRESSURE-TEMPERATURE LIMITS

The pressure-temperature limits of the reactor coolant pressure boundary (RCPB) of Oconee 1 have been established in accordance with the requirements of 10 CFR 50, Appendix G. The methods and criteria employed to establish operating pressure and temperature limits are described in topical report BAW-10046.[8] The objective of these limits is to prevent nonductile failure during any normal operating condition, including anticipated operation occurrences and system hydrostatic tests. The loading conditions of interest include the following:

1. Normal operations, including heatup and cooldown.
2. Inservice leak and hydrostatic tests.
3. Reactor core operation.

The major components of the RCPB have been analyzed in accordance with 10 CFR 50, Appendix G. The closure head region, the reactor vessel outlet nozzle, and the beltline region have been identified as the only regions of the reactor vessel, and consequently of the RCPB, that regulate the pressure-temperature limits. Since the closure head region is significantly stressed at relatively low temperatures (due to mechanical loads resulting from bolt preload), this region largely controls the pressure-temperature limits of the first several service periods. The reactor vessel outlet nozzle also affects the pressure-temperature limit curves of the first several service periods. This is due to the high local stresses at the inside corner of the nozzle, which can be two to three times the membrane stresses of the shell. After the first several years of neutron radiation exposure, the RT_{NDT} of the beltline region materials will be high enough that the beltline region of the reactor vessel will start to control the pressure-temperature limits of the RCPB. For the service period for which the limit curves are established, the maximum allowable pressure as a function of fluid temperature is obtained through a point-by-point comparison of the limits imposed by the closure head region, the outlet nozzle, and the beltline region. The maximum allowable pressure is taken to be the lowest of the three calculated pressures.

The eighth full-power year was selected because the estimated third surveillance capsule will be withdrawn at the end of the refueling cycle when the fluence corresponds to approximately the ninth full-power year. The time difference between the withdrawal of the second and third surveillance capsule provides adequate time for re-establishing the operating pressure and temperature limits for the period of operation between the third and fourth surveillance capsule withdrawals.

The limit curves for Oconee 1 are based on the predicted values of the adjusted reference temperatures of all the beltline region materials at the end of the sixth full-power year. The unirradiated impact properties were determined for the surveillance beltline region materials in accordance with 10 CFR 50, Appendixes G and H. For the other beltline region and RCPB materials, the unirradiated impact properties were estimated using the methods described in BAW-10046P.[8] The unirradiated impact properties and residual elements of the beltline region materials are listed in Table A-1. The adjusted reference temperatures are calculated by adding the predicted radiation-induced ΔRT_{NDT} and the unirradiated RT_{NDT}. The predicted ΔRT_{NDT} is calculated using the respective neutron fluence and copper and phosphorous contents. Figure 8-1 illustrates the calculated peak neutron fluence at several locations through the reactor vessel beltline region wall and at the center of the surveillance capsules as a function of exposure time. The supporting information for Figure 8-1 is described in BAW-10100.[9] The neutron fluence values of Figure 8-1 are the predicted fluences, which have been demonstrated (section 6) to be conservative. The design curves of Regulatory Guide 1.99* were used to predict the radiation-induced ΔRT_{NDT} values as a function of the material's copper and phosphorus content and neutron fluence.

The neutron fluences and adjusted RT_{NDT} values of the beltline region materials at the end of the sixth full-power year are listed in Table 8-1. The neutron fluences and adjusted RT_{NDT} values are given for the 1/4T and 3/4T vessel wall locations (T = wall thickness). The assumed RT_{NDT} of the closure head region and the outlet nozzle steel forgings is 60F, in accordance with BAW-10046P.[8]

Figure 8-2 shows the reactor vessel's pressure-temperature limit curve for normal heatup. This figure also shows the core criticality limits as required

- - - - -

*Revision 1, January 1976.

by 10 CFR 50, Appendix G. Figures 8-3 and 8-4 show the vessel's pressure-temperature limit curve for normal cooldown and for heatup during inservice leak and hydrostatic tests, respectively. All pressure-temperature limit curves are applicable up to the seventh effective full-power year. Protection against nonductile failure is ensured by maintaining the coolant pressure below the upper limits of the pressure-temperature limit curves. The acceptable pressure and temperature combinations for reactor vessel operation are below and to the right of the limit curve. The reactor is not permitted to go critical until the pressure-temperature combinations are to the right of the criticality limit curve. To establish the pressure-temperature limits for protection against nonductile failure of the RCPB, the limits presented in Figures 8-2 through 8-4 must be adjusted by the pressure differential between the point of system pressure measurement and the pressure on the reactor vessel controlling the limit curves. This is necessary because the reactor vessel is the most limiting component of the RCPB.

Table 8-1. Data for Preparation of Pressure-Temperature Limit Curves for Oconee Unit 1, Applicable Through 8 EFPY

Material identif'n		Beltline region location	Core midplane to weld CL, cm	Loc'n from major axis, °	Welds 1/4T loc'n	Unirr RT_{NDT}, F	Content		Neutron fluence at end of 8 EFPY (E > 1 MeV), n/cm²		Radiation-induced ΔRT_{NDT} at end of 8 EFPY, F		Adjusted RT_{NDT} at end of 8 EFPY, F	
Heat No.	Type						Cu, %	P, %	At 1/4T	At 3/4T	At 1/4T	At 3/4T	At 1/4T	At 3/4T
AHR 54	SA508 Cl 2	Lower nozzle belt	--	--	--	(+60)	0.16	0.006	3.44E+17	1.18E+16	22	4	82	64
C-2197-2	SA302 Mod	Interm shell	--	--	--	(+40)	0.10	0.009	2.56E+18	6.1E+17	33	16	73	56
C-3278-1	SA302 Mod	Upper shell	--	--	--	(+40)	0.18	0.010	2.56E+18	6.1E+17	76	37	116	77
C-3265-1	SA302 Mod	Upper shell	--	--	--	20	0.13	0.015	2.56E+18	6.1E+17	63	31	83	51
C-2800-1	SA302 Mod	Lower shell	--	--	--	(+40)	0.14	0.012	2.56E+18	6.1E+17	61	30	101	70
C-2800-2	SA302 Mod	Lower shell	--	--	--	20	0.14	0.012	2.56E+18	6.1E+17	61	30	81	50
SA-1494	Weld	Outlet nozzle weld	+245	--	--	(+20)	0.14	0.015	8.5E+16	--	13	--	33	--
SA-1526	Weld	Outlet nozzle weld	+245	--	--	(+20)	0.46	0.016	8.5E+16	--	41	--	61	--
SA-1135	Weld	Interm circ	+199	--	Yes	(+20)	0.17	0.015	5.64E+17	1.36E+16	29	5	49	25
SA-1229	Weld	Upper circ (61%)	+123	--	Yes	(+20)	0.20	0.021	2.56E+18	6.1E+17	114	56	134	76
WF-25	Weld	Upper circ (39%)	+123	--	No	(+20)	0.29	0.019	--	6.1E+17	--	75	--	95
SA-1585	Weld	Middle circ	-61	--	Yes	(+20)	0.25	0.016	2.56E+18	6.1E+17	127	62	147	82
WF-9	Weld	Lower circ	-249	--	Yes	(+20)	0.17	0.015	8.5E+16	--	15	--	35	--
SA-1073	Weld	Upper long.	--	--	Yes	(+20)	0.21	0.025	1.63E+18	3.65E+17	103	49	123	69
SA-1493	Weld	Middle long.	--	48	Yes	(+20)	0.22	0.017	1.59E+18	3.65E+17	90	43	110	63
SA-1430	Weld	Lower long.	--	20	Yes	(+20)	0.16	0.017	2.11E+18	4.79E+17	76	36	96	56

Figure 8-1. Fast Neutron Fluence of Surveillance Capsule Center Compared to Various Locations Through Reactor Vessel Wall for First 10 EFPY

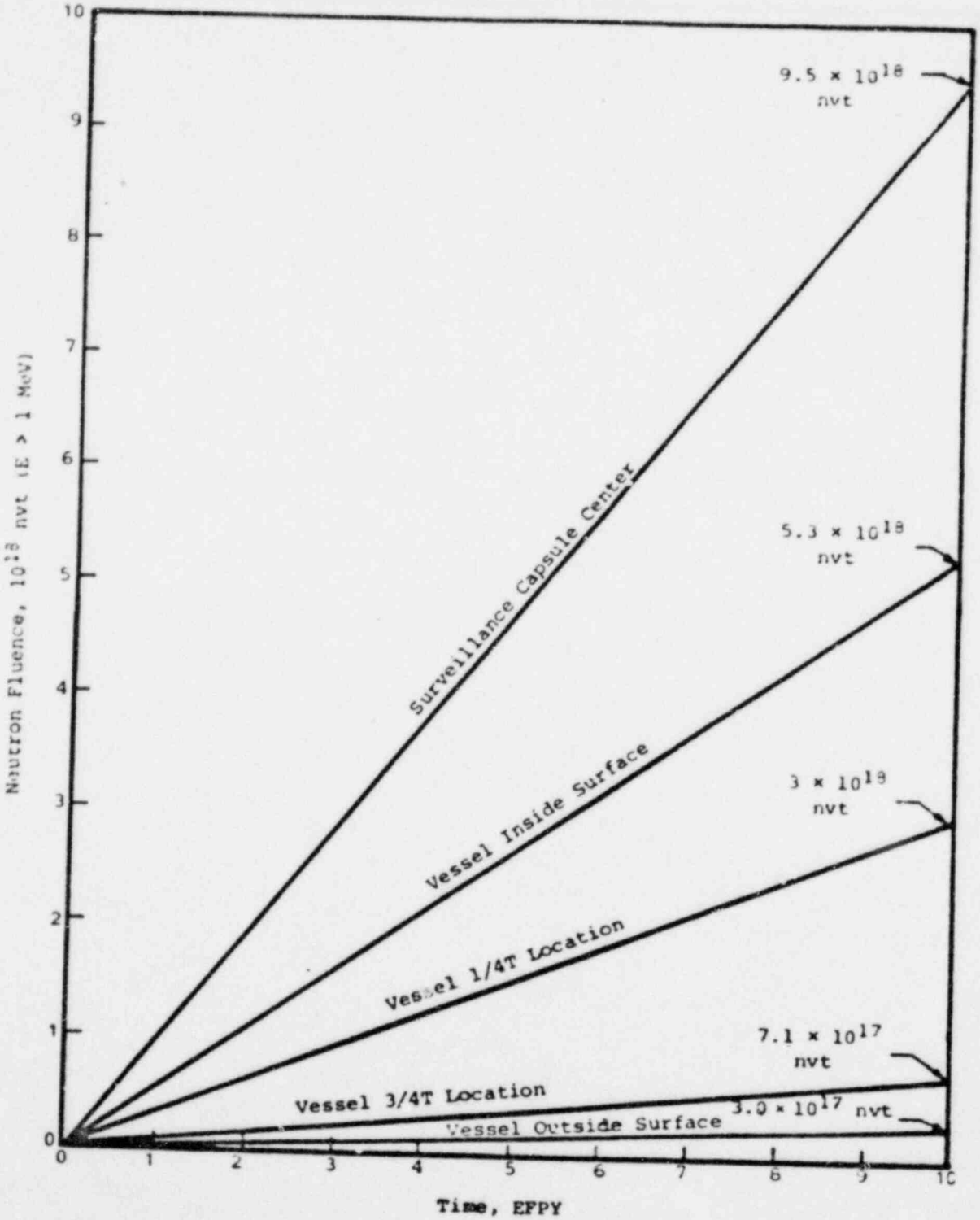

Figure 8-2. Reactor Vessel Pressure-Temperature Limit Curves for Normal Operation Heatup Applicable for First 8 EFPY

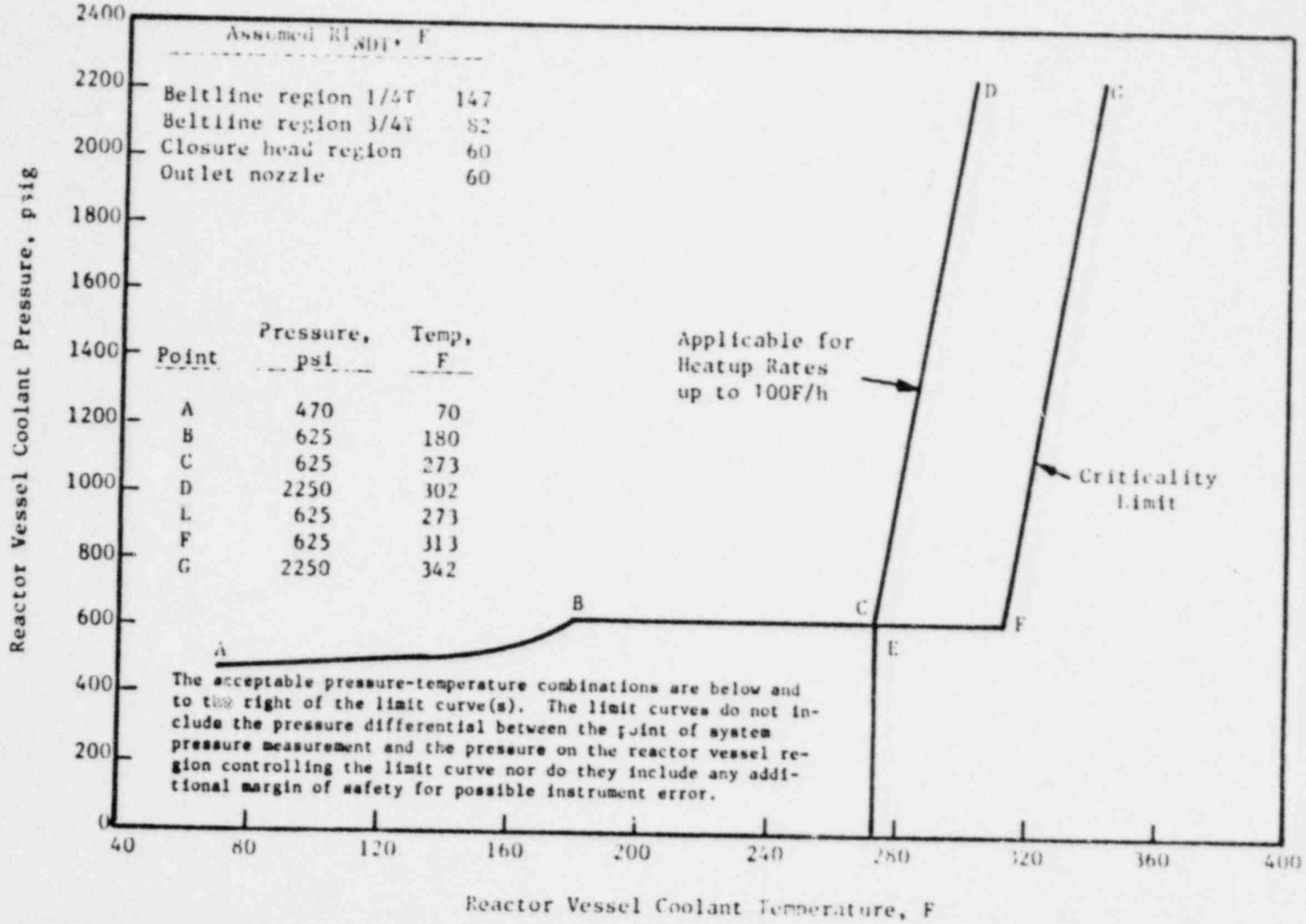

Figure 8-3. Reactor Vessel Pressure-Temperature Limit Curve for Normal Operation – Cooldown Applicable for First 8 EFPY

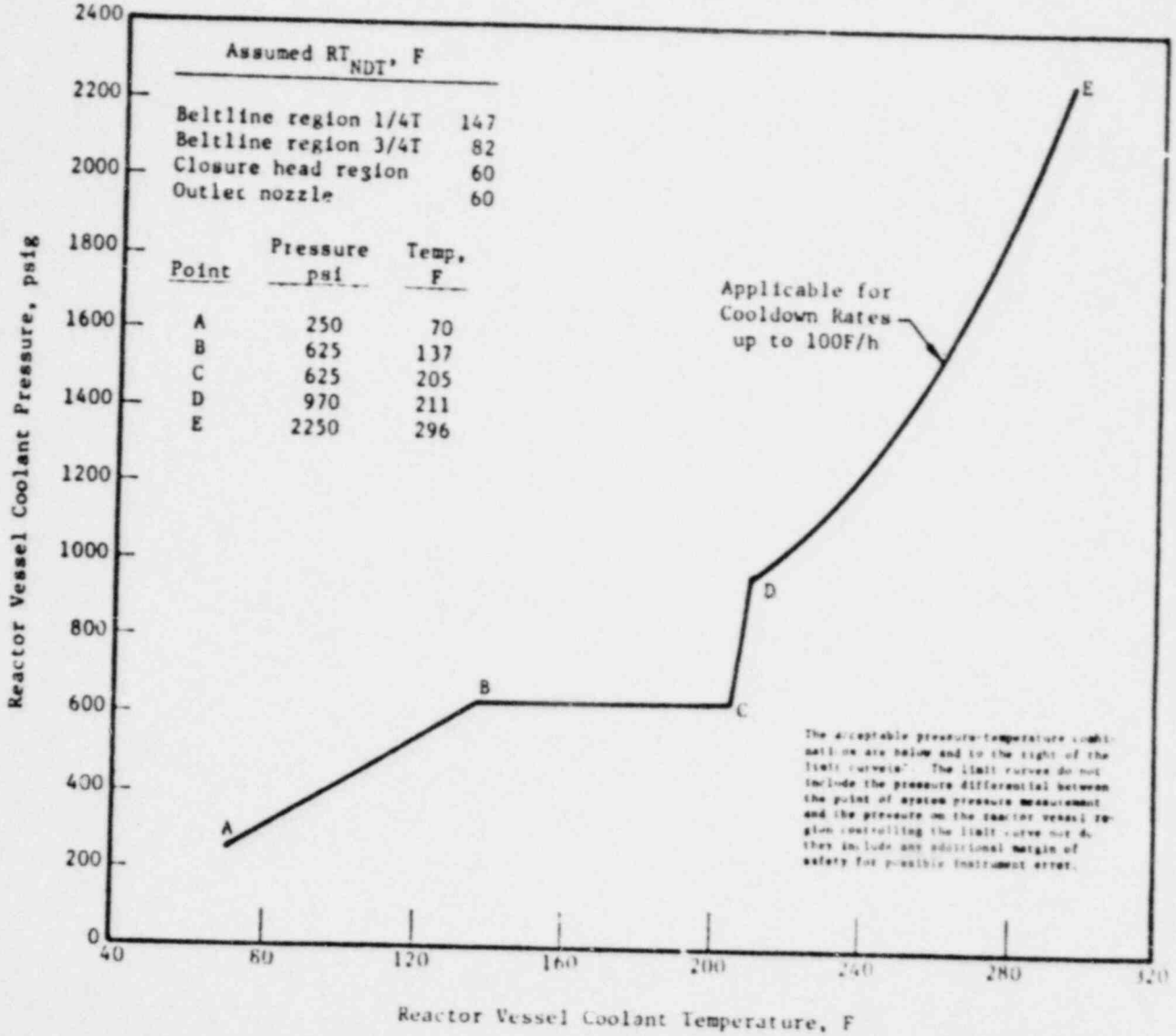

Figure 8-4. Reactor Vessel Pressure-Temperature Limit Curve for Inservice Leak and Hydrostatic Tests, Applicable for First 8 EFPY

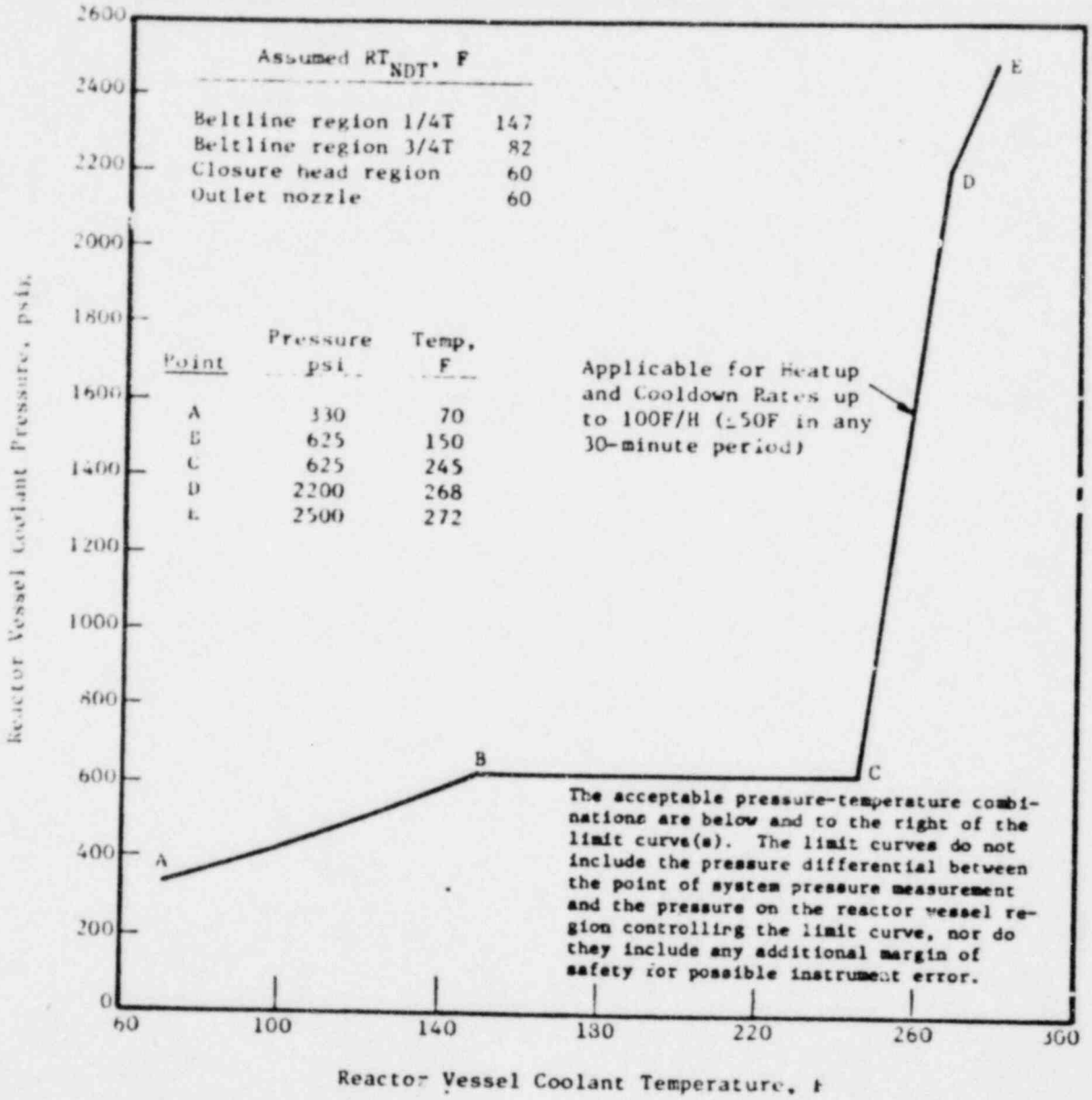

9. SUMMARY OF RESULTS

The analysis of the reactor vessel material contained in the first surveillance capsule OCI-E removed from the Oconee 1 pressure vessel led to the following conclusions:

1. The capsule received an average fast fluence of 1.5×10^{18} n/cm^2 (E > 1 MeV). The predicted fast fluence for the reactor vessel T/4 location at the end of the second fuel cycle is 4.9×10^{17} n/cm^2 (E > 1 MeV).

2. The fast fluence of 1.5×10^{18} n/cm^2 (E > 1 MeV) increased the RT_{NDT} of the capsule reactor vessel core region shell materials to a maximum of 124F.

3. Based on a ratio of 1.6 between the fast flux at the surveillance capsule location to that at the vessel wall and an 80% load factor, the projected fast fluence that the Oconee 1 reactor pressure vessel will receive in 40 calendar years' operation is 1.8×10^{19} n/cm^2 (E > 1 MeV).

4. The increase in the RT_{NDT} for the base plate material was in good agreement with that predicted by the currently used design curves of ΔRT_{NDT} versus fluence.

5. The increase in the RT_{NDT} for the weld metal was in good agreement with that predicted by the currently used design curves of ΔRT_{NDT} versus fluence.

6. The current techniques used for predicting the change in Charpy impact upper shelf properties due to irradiation are conservative.

7. The analysis of the neutron dosimeters demonstrated that the analytical techniques used to predict the neutron flux and fluence were accurate.

8. The thermal monitors indicated that the capsule design was satisfactory for maintaining the specimens within the desired temperature range.

10. SURVEILLANCE CAPSULE REMOVAL SCHEDULE

Based on the postirradiation test results of capsule OCI-E, the following schedule is recommended for examination of the remaining capsules in the Oconee 1 reactor vessel surveillance program:

Capsule ID	Evaluation schedule: Est. capsule fluence, 10^{19} n/cm^2	Est. EFPD: Surface	Est. EFPD: 1/4T	Est. date[c] data available
OCI-A[a]	1.2	18	32	1984
OCI-C[a]	2.3	34	61	1988
OCI-B	Standby	--	--	--
OCI-D	Standby	--	--	--
OCI-G[a,b]	Standby	--	--	--
OCI-H[b]	Standby	--	--	--

[a] Capsules contain weld metal specimens.

[b] Capsules designated thermal aging capsules.

[c] These dates do not represent the earliest dates that data will be available for the materials that control the operating limitations. Similar materials are included as part of the B&W Integrated Reactor Surveillance Program, which will provide necessary data on a timely basis. The earliest date that these data will be available is 1980.

11. CERTIFICATION

The specimens were tested, and the data obtained from Oconee Nuclear Station, Unit 1 surveillance capsule OCI-E were evaluated using accepted techniques and established standard methods and procedures in accordance with the requirements of 10 CFR 50, Appendixes G and H.

A. L. Lowe, Jr., P.E. — Date: 27 Sept 1977
Project Technical Manager

This report has been reviewed for technical content and accuracy.

K. E. Moore — Date: 9-27-77
Technical Staff

12. REFERENCES

1. A. L. Lowe, Jr., et al., Analysis of Capsule OC1-E From Duke Power Company Oconee Unit 1 Reactor Vessel Materials Surveillance Program, BAW-1421, Rev. 1 Babcock & Wilcox, Lynchburg, Virginia, September 1975.

2. G. J. Snyder and G. S. Carter, Reactor Vessel Material Surveillance Program, BAW-10006A, Rev. 3, Babcock & Wilcox, Lynchburg, Virginia, January 1975.

3. User's Manual for ANISN, a One-Dimensional Discrete Ordinates Transport Code With Anisotropic Scattering, K-1693 (RSIC-CCC-82), Union Carbide Corp., Nuclear Division, March 1967.

4. User's Manual for the DOT-IIW Discrete Ordinates Transport Computer Code, WANL-TME-1982, December 1969.

5. CASK — 40-Group Coupled Neutron and Gamma-Ray Cross Section Data, RSIC-DLC-23, Radiation Shielding Information Center.

6. Draft — New Standard E482-00, "Recommended Practice for Neutron Dosimetry for Reactor Pressure Vessel Surveillance," October 10, 1974.

7. H. S. Palme, G. S. Carter, and C. L. Whitmarsh, Reactor Vessel Material Surveillance Program — Compliance With 10 CFR 50, Appendix H, for Oconee-Class Reactors, BAW-10100A, Babcock & Wilcox, Lynchburg, Virginia, February 1975.

8. H. S. Palme and H. W. Behnke, Methods of Compliance With Fracture Toughness and Operational Requirements of Appendix G to 10 CFR 50, BAW-10046P, Babcock & Wilcox, Lynchburg, Virginia, October 1975.

APPENDIX A

Reactor Vessel Surveillance Program -- Background Data and Information

1. Material Selection Data

The data used to select the materials for the specimens in the surveillance program, in accordance with E-185-66, are shown in Table A-1. The locations of these materials within the reactor vessel are shown in Figures A-1 and A-2.

2. Definition of Beltline Region

The beltline region of Oconee Nuclear Unit 1 was defined in accordance with the data given in BAW-10100A.

3. Capsule Identification

The capsules used in the Oconee Nuclear Unit 1 surveillance program are identified below by identification number, type, and location.

Capsule Cross Reference Data

Number	Type	Location
OCI-A	A	Upper
OCI-B	B	Lower
OCI-C	A	Upper
OCI-D	B	Lower
OCI-E	A	Upper
OCI-F	B	Lower
OCI-G	A	Thermal aging
OCI-H	B	Thermal aging

4. Specimens per Surveillance Capsule

See Tables A-2 and A-3.

Table A-1. Surveillance Program Materials Selection Data for Oconee 1

Material ID, heat No.	Material type	Beltline region location	Distance core mid-plane to weld center-line, cm	Drop weight T_{NDT}, F	Charpy data, C_{VN}					Chemistry			
						Transverse							
					Long., ft-lb @ 10F	50-ft-lb, F	35 MLE, F	USE, ft-lb	RT_{NDT}, F	Cu, %	P, %	Si, %	Ni, %
AHR 54	SA50E, Cl 2	Nozzle belt	--	--	{80, 95, 107} {87, 54, 112}	--	--	--	--	0.15	0.006	0.010	--
C-2197-2	SA302 B	Interm shell	--	--	39, 45, 26	--	--	--	--	0.10	0.009	0.010	--
C-3278-1	SA302 B	Upper shell	--	<10	35, 29, 53	--	--	--	--	0.12	0.010	0.016	--
C-3265-1	SA302 B	Upper shell	--	0	34, 64, 27	--	--	109	20	0.15	0.015	0.015	--
C-2800-1	SA302 B	Lower shell	--	<10	34, 39, 39	--	--	--	--	0.11	0.012	0.017	--
C-2800-2	SA302 B	Lower shell	--	20	32, 33, 49	--	--	119	20	0.11	0.012	0.017	--
SA-1430	Weld	Long seam	--	--	54, 52, 53	--	--	--	--	0.16	0.017	0.015	--
SA-1493	Weld	Long seam	--	--	41, 35, 40	--	--	--	--	0.22	0.017	0.010	--
SA-1073	Weld	Long seam	--	--	40, 45, 39	--	--	--	--	0.21	0.025	0.017	--
WF-9	Weld	Circ seam	-249	--	46, 43, 45	--	--	--	--	0.17	0.015	0.012	--
SA-1585	Weld	Circ seam	-61	--	31, 32, 31	--	--	--	--	0.25	0.016	0.011	--
WF-25	Weld	Circ seam	+123	-40	38, 28, 49	--	--	82	9	0.29	0.019	0.010	--
SA-1229	Weld	Circ seam	+123	--	55, 45, 40	--	--	--	--	0.20	0.021	0.012	--
SA-1135	Weld	Circ seam	+199	--	56, 44, 55	--	--	--	--	0.17	0.015	0.013	--
SA-1526	Weld	Circ seam	+245	--	33, 33, 33	--	--	--	--	0.36	0.016	0.012	--
SA-1494	Weld	Circ seam	+245	--	54, 25, 44	--	--	--	--	0.14	0.015	0.012	--

Table A-2. Materials and Specimens in Upper Surveillance Capsules OCI-A, OCI-C, and OCI-E

Material description	No. of specimens	
	Tensile	Charpy
Weld metal, WF-112	4	8
Heat-affected zone (HAZ)		
Heat A — C-3265-1, longitud	0	8
Baseline material		
Heat A — C-3265-1, longitud	4	8
Heat A — C-3265-1, transverse	0	4
Correlation HSST plate 02	0	8
Total per capsule	8	36

Table A-3. Materials and Specimens in Lower Surveillance Capsules OCI-B, OCI-D, and OCI-F

Material description	No. of specimens	
	Tensile	Charpy
Heat-affected zone (HAZ)		
Heat B — 2800-2, longitud	4	10
Baseline material		
Heat B — C-2800-2, longitud	4	10
Heat B — C-2800-2, transverse	0	8
Correlation HSST plate 02	0	8
Total per capsule	8	36

Figure A-1. Location and Identification of Materials Used in Fabrication of Oconee Unit 1 Reactor Pressure Value

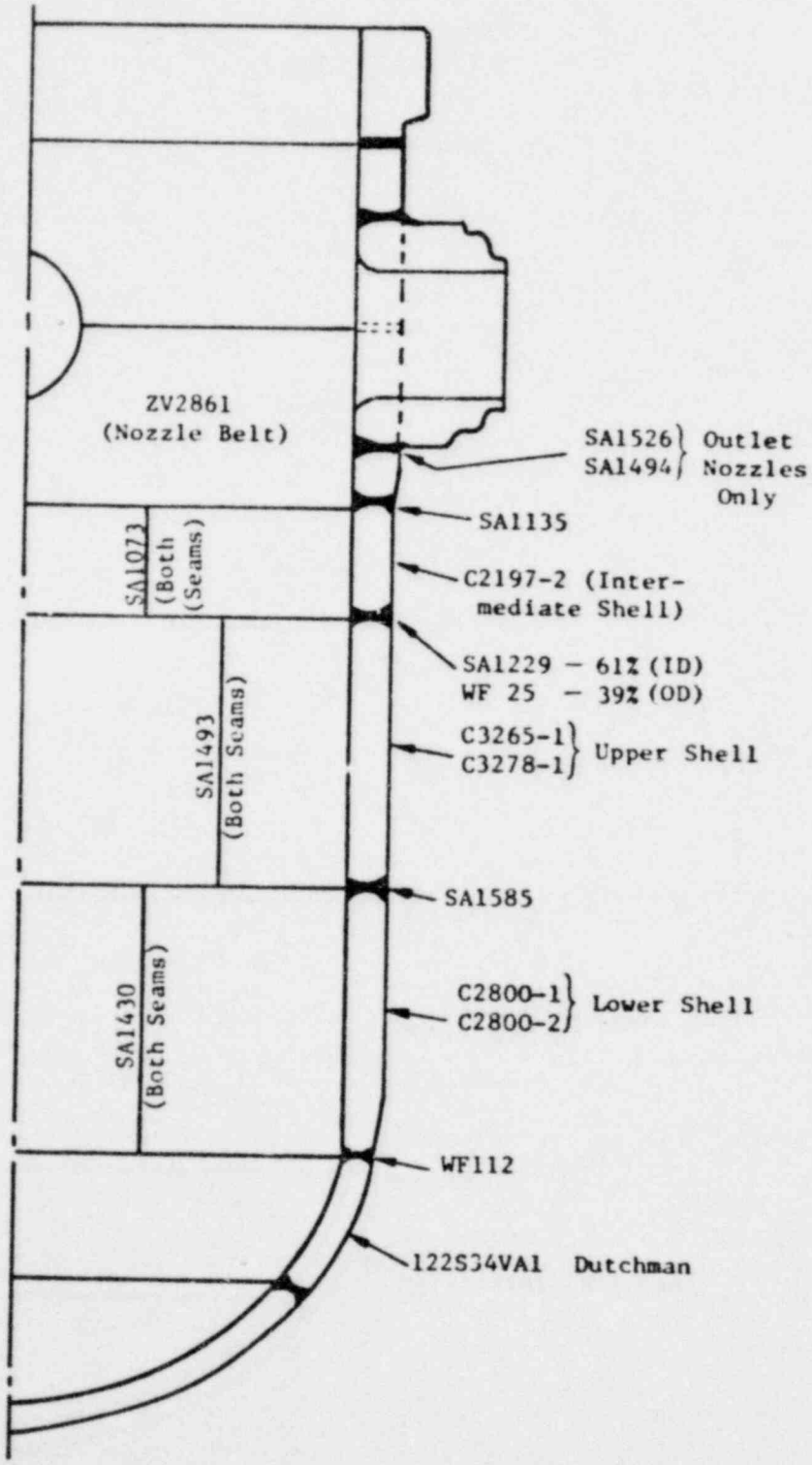

Figure A-2. Location of Longitudinal Welds in Upper, Lower, and Intermediate Shell Courses

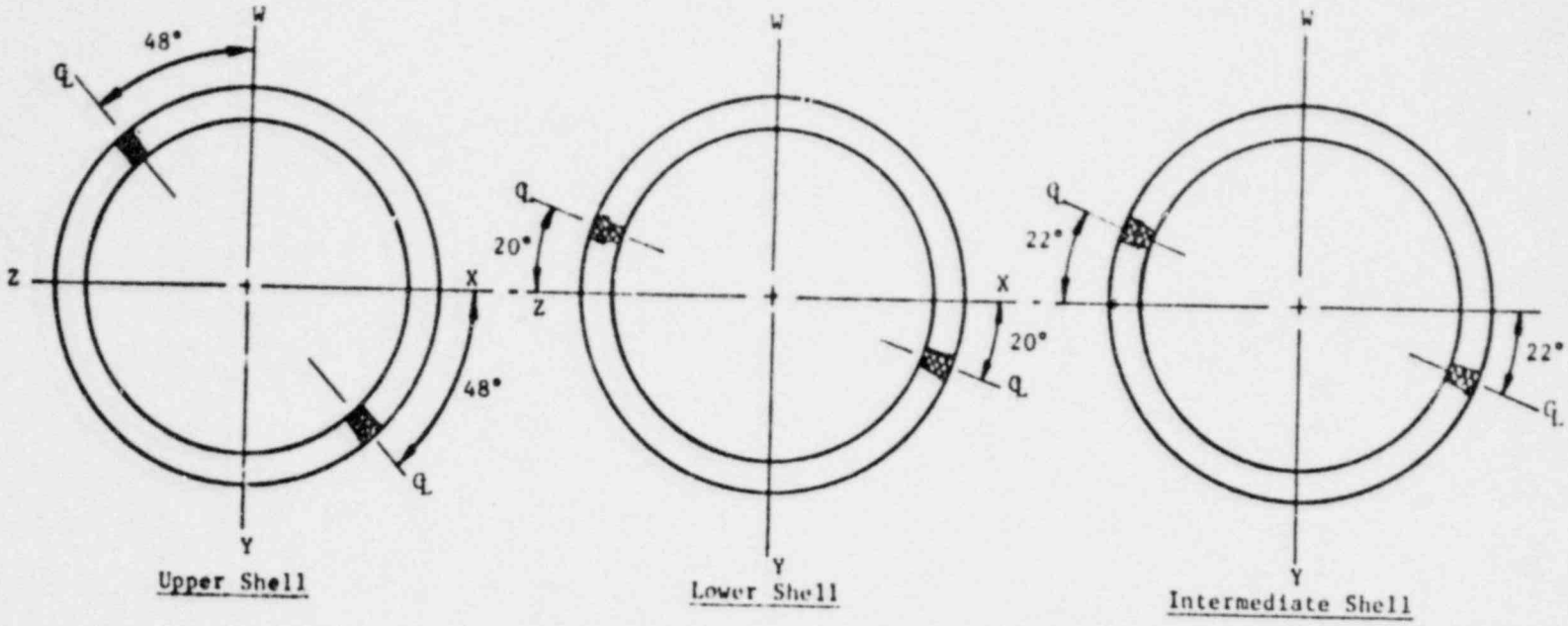

APPENDIX B

Preirradiation Tensile Data

Table B-1. Preirradiation Tensile Properties of Shell Plate Material, Heat C-3265-1

Specimen No.	Test temp, F	Strength, psi		Elongation, %		Red'n of area, %
		Yield	Ult.	Unif.	Total	
Longitudinal						
AA-701	RT	64,000	85,900	15.1	28.9	63.0
705	RT	64,200	85,900	ND	27.8	71.0
723	RT	64,700	86,300	14.9	22.8	71.0
Mean, $\bar{X}$	--	64,300	86,100	15.0	26.5	68.0
Std dev'n	--	299.3	213.8	0.163	3.24	4.0
AA-706	600	56,900	83,200	15.1	26.4	68.0
710	600	57,800	85,200	16.3	27.1	68.0
715	600	59,200	84,800	15.0	28.5	73.0
Mean, $\bar{X}$	--	58,000	84,400	15.5	27.3	70.01
Std dev'n	--	1,170	1,050	0.72	1.09	2.625
Transverse						
AA-601	RT	65,100	86,600	14.6	26.0	63.0
606	RT	65,500	86,900	14.5	27.8	67.0
607	RT	64,700	86,100	16.1	24.6	65.0
Mean, $\bar{X}$	--	65,100	86,500	15.1	26.1	65.0
Std dev'n	--	400.1	408.1	0.89	1.61	2.1
AA-604	600	57,800	84,500	15.7	25.4	63.0
605	600	57,100	83,400	16.0	26.1	63.0
609	600	58,900	84,800	14.2	26.1	67.0
Mean, $\bar{X}$	--	57,900	84,200	15.3	25.8	64.0
Std dev'n	--	905.2	708.8	0.93	0.37	2.4

Table B-2. Preirradiation Tensile Properties of Shell Plate Material, HAZ, Heat C-3265-1

Specimen No.	Test temp, F	Strength, psi		Elongation, %		Red'n of area, %
		Yield	Ult.	Unif.	Total	
Longitudinal						
AA-406	RT	60,700	79,500	10.9	21.6	64.0
407	RT	63,700	81,800	11.2	22.6	62.0
409	RT	60,600	79,900	11.5	29.5	64.0
Mean, $\bar{X}$	--	61,600	80,400	11.2	24.6	63.0
Std dev'n	--	1,750	1,300	0.29	4.30	1.0
AA-401	600	56,100	81,800	12.2	20.0	53.0
404	600	57,700	81,200	12.3	21.0	47.0
408	600	56,800	80,400	11.1	19.6	52.0
Mean, $\bar{X}$	--	56,900	81,100	11.9	20.2	51.0
Std dev'n	--	795.4	725.4	0.08	0.72	3.2
Transverse						
AA-302	RT	65,600	86,400	14.4	27.8	70.0
303	RT	64,900	86,300	15.2	29.2	71.0
304	RT	69,000	89,700	14.3	29.0	74.0
Mean, $\bar{X}$	--	66,500	87,500	14.7	28.7	72.0
Std dev'n	--	2,210	1,910	0.49	0.75	2.0
AA-305	600	57,100	83,600	16.3	30.0	72.0
306	600	55,200	85,300	15.8	31.4	68.0
301	600	58,500	86,800	13.7	25.2	70.0
Mean, $\bar{X}$	--	56,900	85,300	15.3	28.8	70.0
Std dev'n	--	1,620	1,620	1.33	3.24	1.9

Table B-3. Preirradiation Tensile Properties of Weld Metal, Weld Qualification No WF112

Specimen No.	Test temp, F	Strength, psi		Elongation, %		Red'n of area, %
		Yield	Ult	Unif.	Total	
Longitudinal						
OCI-105	RT	63,900	81,100	17.2	32.1	63.0
108	RT	63,400	80,300	16.9	30.7	64 0
123	RT	62,700	80,100	16.6	30.0	64.0
Mean, $\bar{X}$	--	63,300	80,500	16.9	30.9	63.0
Std dev'n	--	625.8	548.4	0.30	1.0	0.5
OCI-118	600	55,300	79,600	16.8	25.0	63.0
121	600	58,400	82,200	16.9	22.9	60.0
124	600	55,500	80,500	16.7	25.3	60.0
Mean, $\bar{X}$	--	56,400	80,800	16.8	24.4	61.0
Std dev'n	--	1763.7	1337.1	0.13	1.32	1.8

APPENDIX C

Preirradiation Charpy Impact Data

Table C-1. Preirradiation Charpy Impact Data for Shell Plate Material, Longitudinal Direction, Heat C-3265-1

Specimen No.	Test temp, F	Absorbe' ener ft-	Lateral expansion, 10^{-3} in.	Shear fracture, %
AA-715	320	139	72	100
724	320	150	64	100
899	320	139	70	100
AA-897	2[illegible]	142	73	100
AA-707	[illegible]	137	66	85
747	[illegible]00	143	73	80
898	200	140	72	80
AA-[illegible]2	131	125	67	75
749	131	110	62	80
AA-731	67	98	46	45
735	67	88	38	35
744	67	82	60	15
AA-718	33	67	55	10
736	35	57	46	5
752	35	69	66	12
AA-725	0	23	18	0
740	0	61	49	0
895	0	32	25	0
AA-896	-30	8	6	0
AA-720	-58	11	7	0
900	-60	8	4	0

Table C-2. Preirradiation Charpy Impact Data for Shell Plate Material, Transverse Direction, Heat C-3261-1

Specimen No.	Test temp, F	Absorbed energy, ft-lb	Lateral expansion, 10^{-3} in.	Shear fracture, %
AA-619	320	106	72	100
631	320	108	74	100
700	320	114	72	100
AA-698	261	103	72	100
699	262	113	72	100
AA-623	200	105	63	85
625	200	98	68	90
696	200	110	74	90
AA-614	170	97	81	95
AA-626	129	87	60	85
695	130	85	59	65
AA-628	100	70	56	30
629	100	65	52	50
AA-604	66	63	49	10
617	66	65	26	15
620	67	42	34	15
AA-601	30	46	37	2
638	30	36	32	2
697	30	36	30	2
AA-624	-40	10	8	1
632	-40	27	20	0

Table C-3. Preirradiation Charpy Impact Data for Shell Material, HAZ, Longitudinal Direction, Heat C-3265-1

Specimen No.	Test temp, F	Absorbed energy, ft-lb	Lateral expansion, 10^{-3} in.	Shear fracture, %
AA-399	320	116	70	100
422	320	114	68	100
428	320	108	74	100
AA-397	262	125	70	100
AA-396	200	117	67	70
401	200	82	58	85
421	200	98	62	90
AA-395	130	108	60	85
427	130	86	57	95
AA-419	67	90	49	85
426	67	90	52	90
442	67	94	52	90
AA-406	30	87	54	55
407	30	71	48	50
414	30	70	52	30
AA-398	20	73	53	35
AA-411	10	63	45	35
AA-400	-20	58	41	15
430	-20	44	30	10
438	-19	35	24	12
AA-429	-59	28	18	5

Table C-4. Preirradiation Charpy Impact Data for Shell Material, HAZ, Transverse Direction, Heat C-3265-1

Specimen No.	Test temp, F	Absorbed energy ft-lb	Lateral expansion, 10^{-3} in.	Shear fracture, %
AA-302	320	100	60	100
304	320	92	62	100
596	320	124	65	100
AA-598	260	102	56	100
AA-303	200	85	59	100
307	200	79	56	100
599	200	111	64	90
AA-301	71	78	48	85
309	67	105	59	100
318	67	92	49	85
AA-310	20	51	40	25
313	20	76	52	55
AA-595	10	68	44	55
AA-308	-20	50	33	15
314	-20	56	37	15
597	-20	38	28	10
AA-319	-45	55	36	5
AA-320	-50	35	25	6
AA-312	-79	21	13	2
316	-79	25	14	1

Table C-5. Preirradiation Charpy Impact Data for Weld Metal, Weld Qualification No. WF 112

Specimen No.	Test temp, F	Absorbed energy, ft-lb	Lateral expansion, 10^{-3} in.	Shear fracture, %
OCI-015	320	68	62	100
016	320	65	55	100
AA-296	320	62	52	100
OCI-004	261	64	59	100
AA-300	260	61	54	100
OCI-030	200	71	55	100
035	200	63	59	98
AA-299	200	63	52	100
AA-298	140	64	57	65
OCI-022	66	57	47	65
025	70	60	41	75
034	70	55	47	60
OCI-011	40	41	39	10
036	40	51	48	45
OCI-020	10	30	28	15
031	11	40	38	20
AA-295	10	37	33	25
OCI-032	-15	33	27	5
OCI-018	-40	19	14	5
023	-40	25	21	5
AA-297	-40	13	14	5

Figure C-1. Impact Data From Unirradiated Base Metal A — Longitudinal Orientation

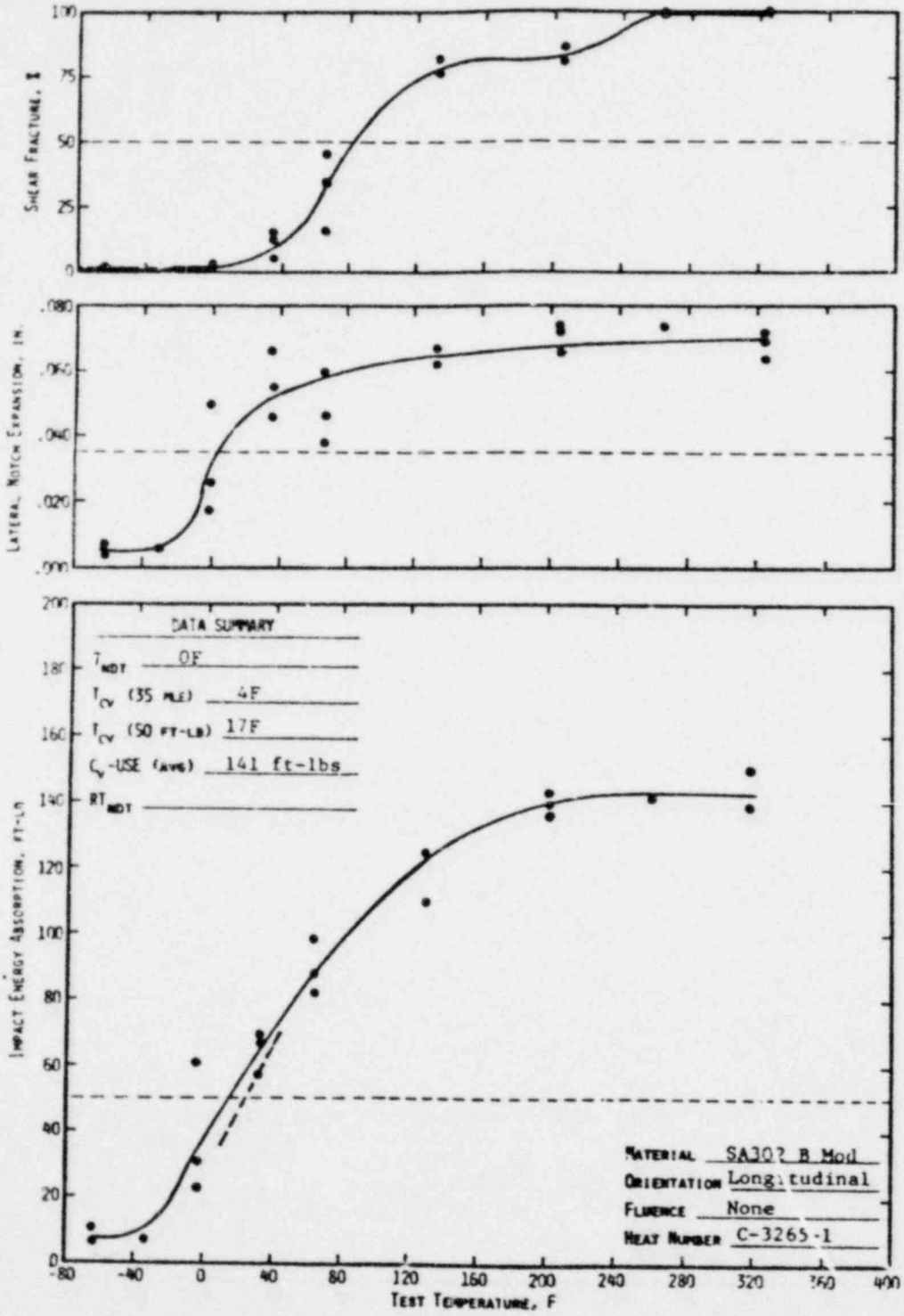

Figure C-2. Impact Data From Unirradiated Base Metal A — Transverse Orientation

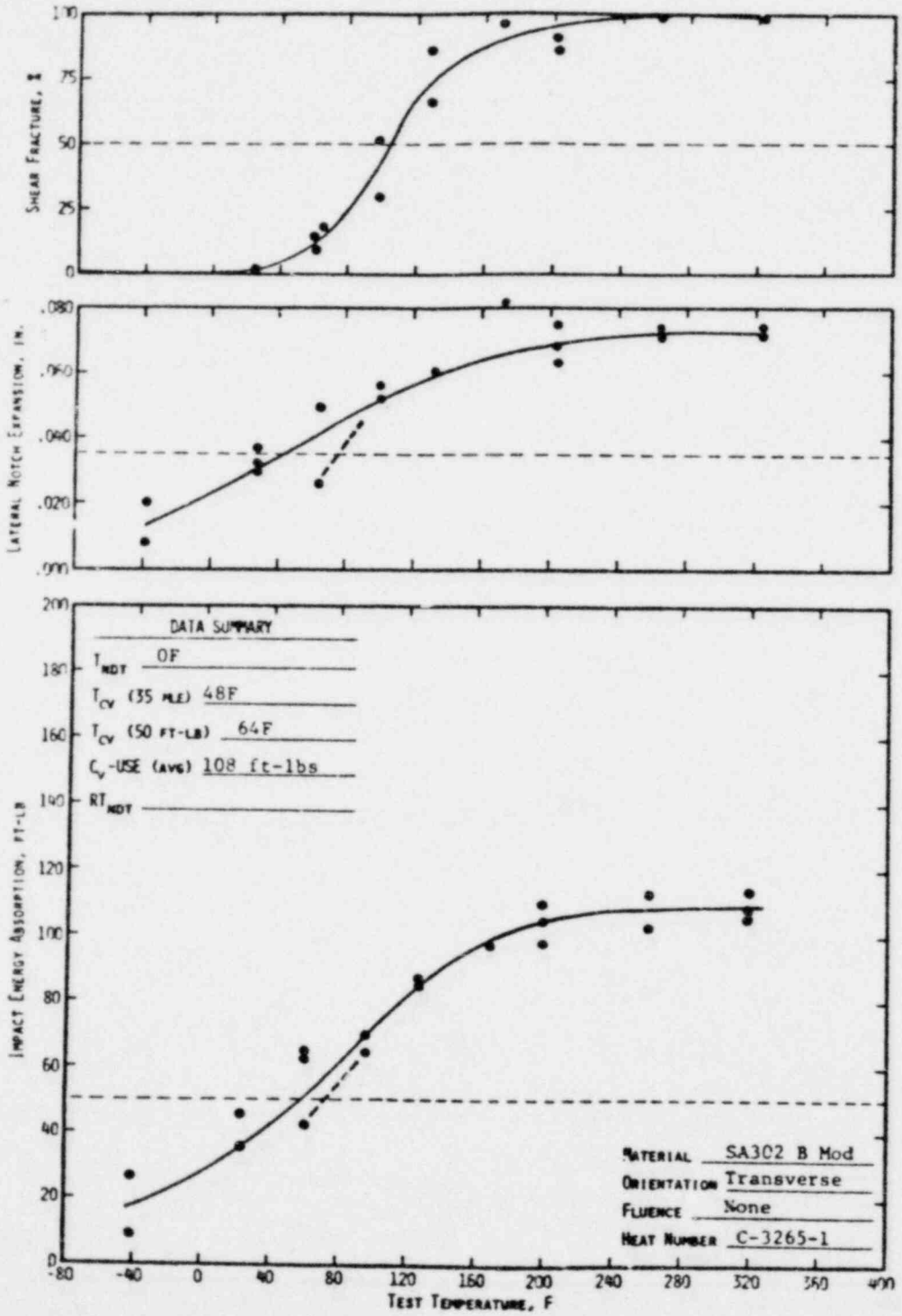

Figure C-3. Impact Data From Unirradiated Base Metal A — HAZ, Longitudinal Orientation

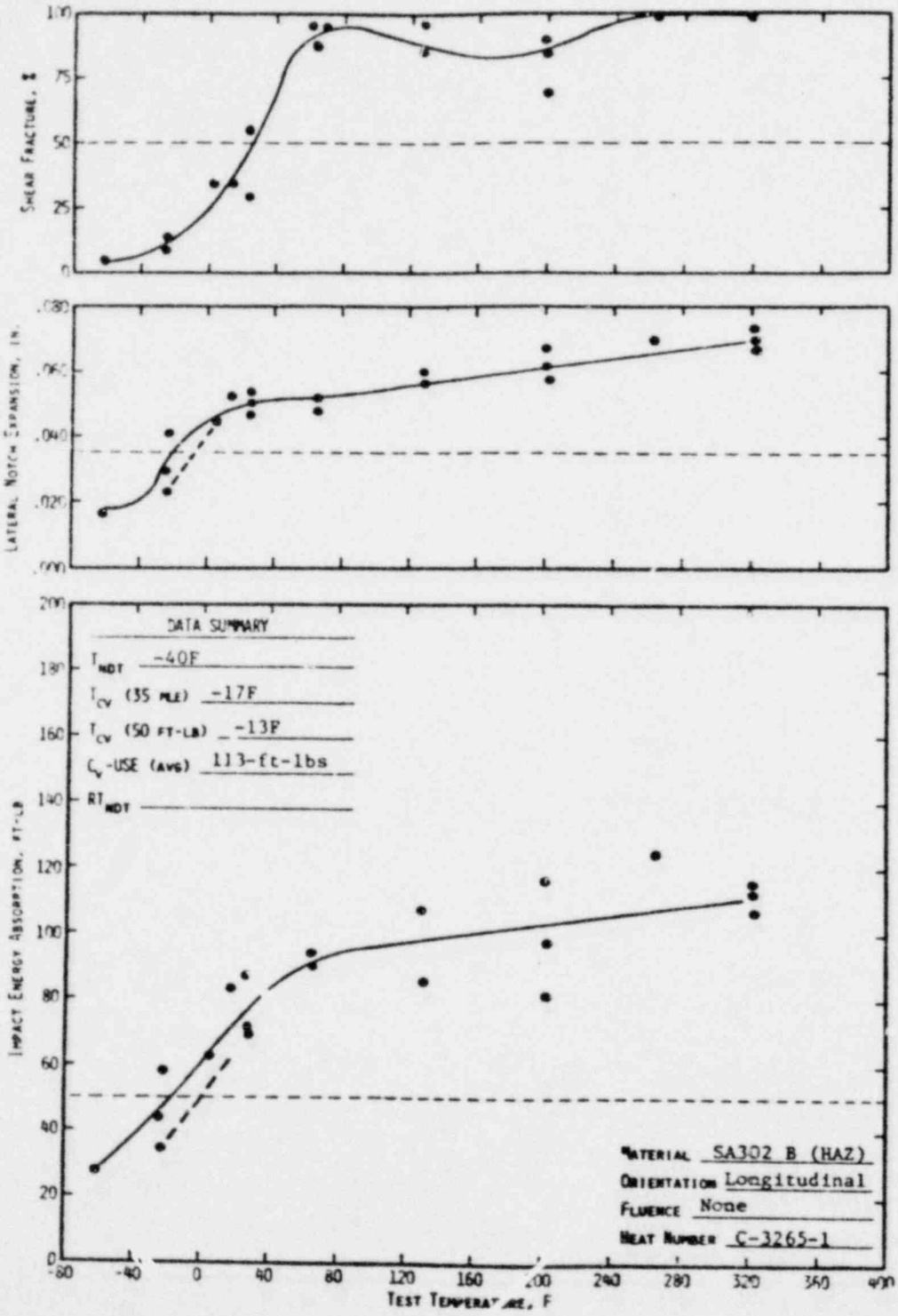

Figure C-4. Impact Data From Unirradiated Base Metal A – HAZ, Transverse Orientation

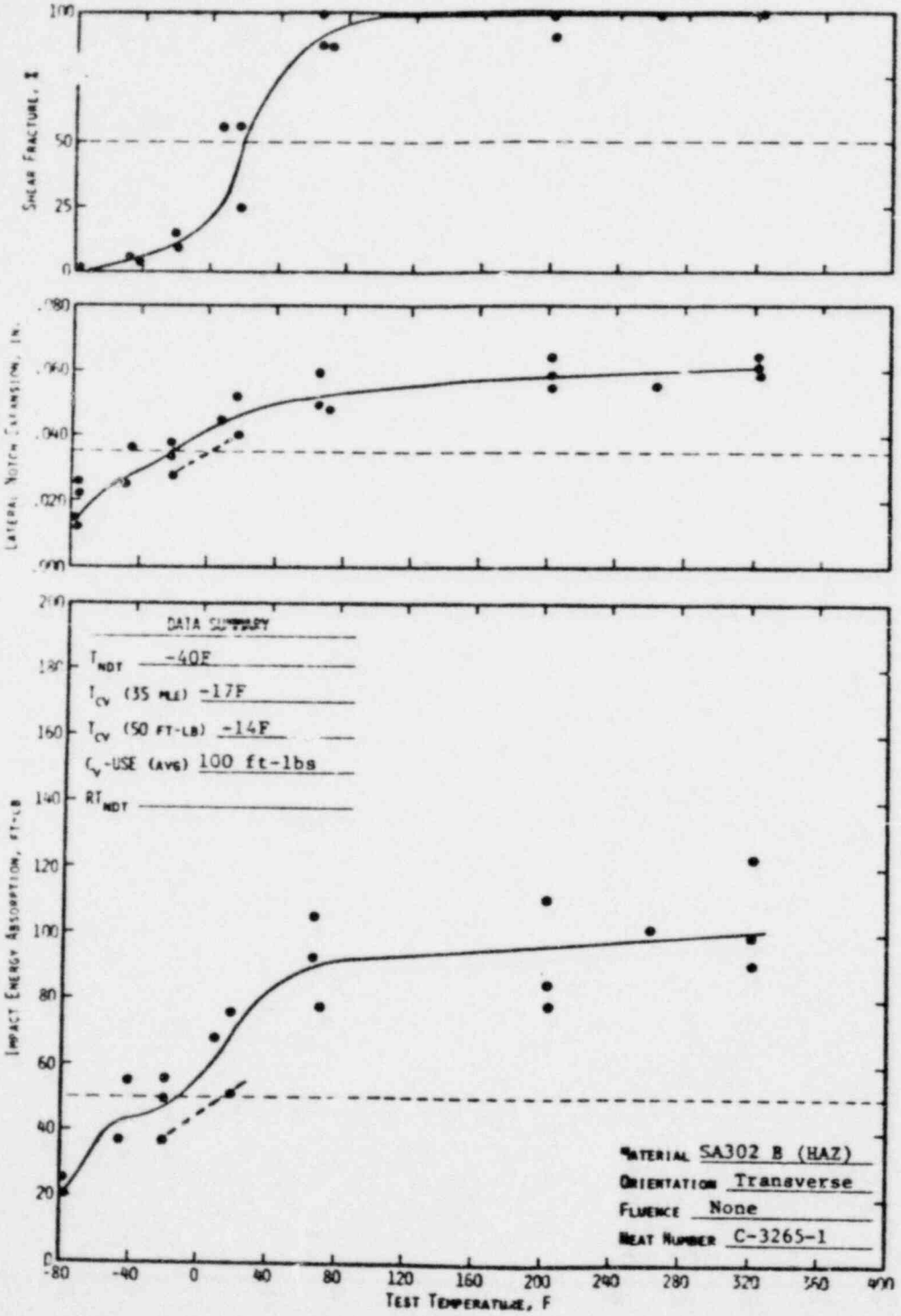

Figure C-5. Impact Data From Unirradiated Weld Metal Longitudinal Orientation

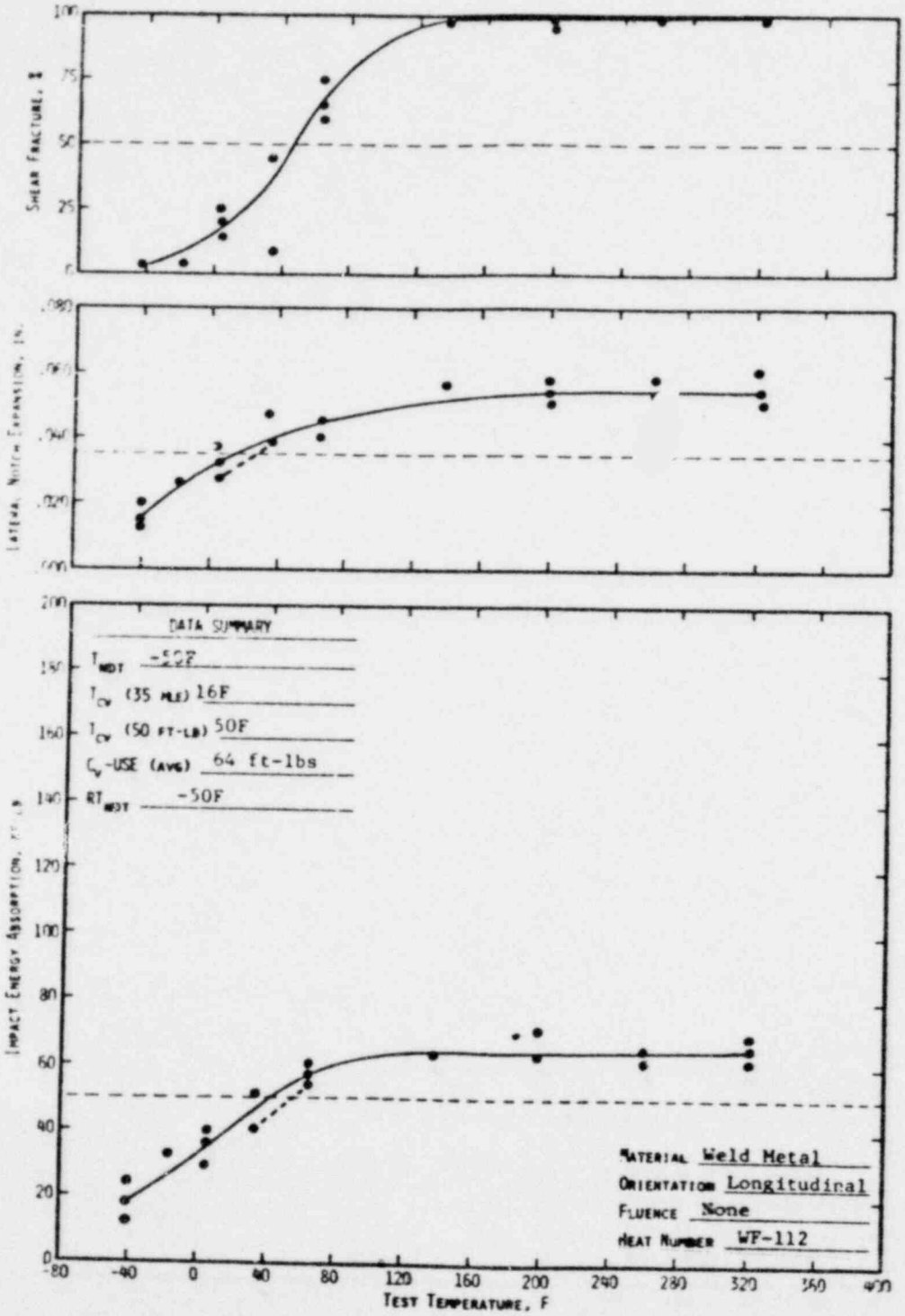

Figure C-6. Impact Data Unirradiated Correlation Material

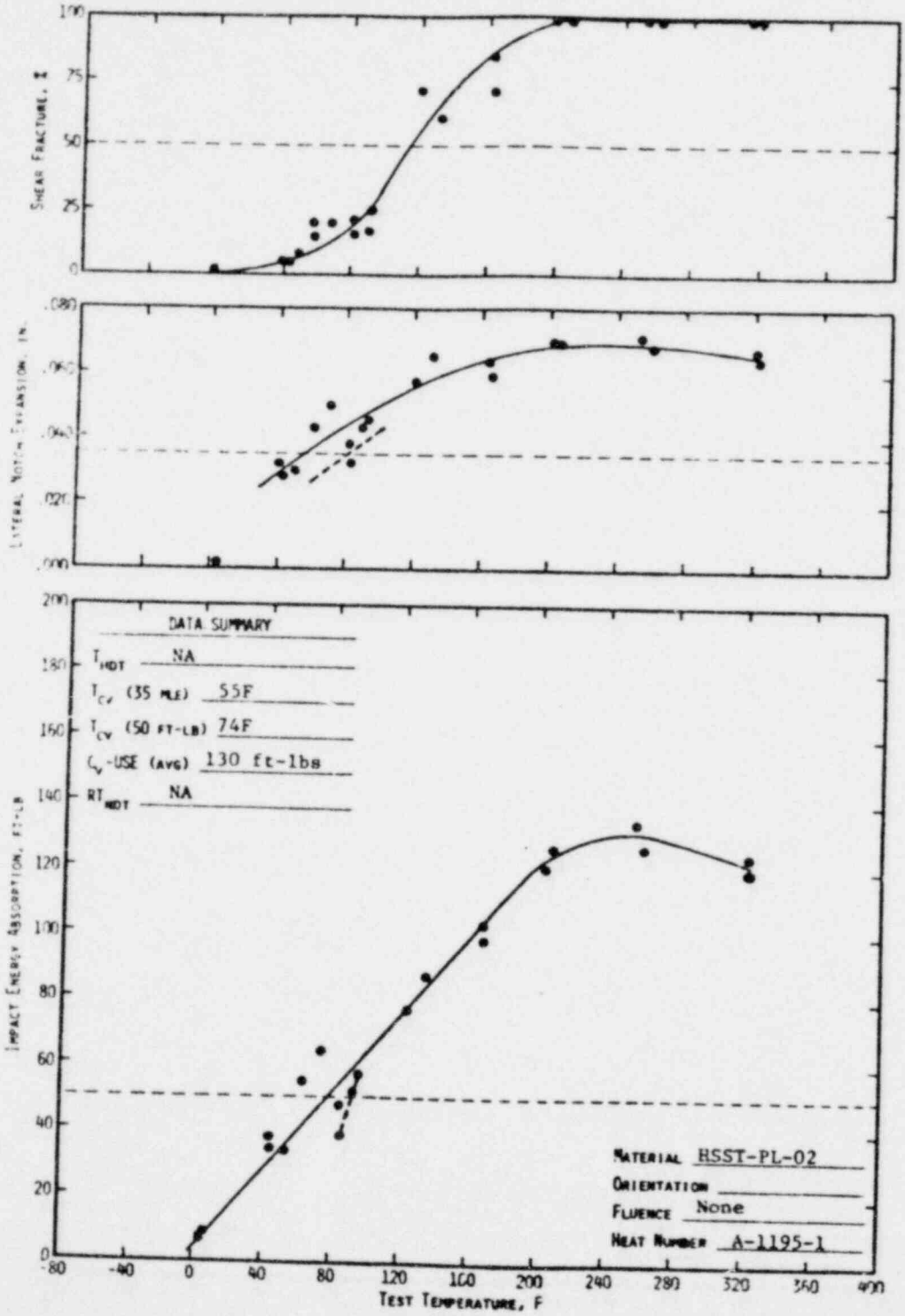

APPENDIX D

Threshold Detector Information

Table D-1 lists the composition of the threshold detectors and the thickness of cadmium used to reduce competing thermal reactions. Table D-2 shows the cycle 1 measured activity per gram of target material (i.e., per gram of uranium, nickel, etc.) corrected for the wait time between irradiation and counting. Measurements after cycle 2 are listed in Table D-3. Activation cross sections for the various target materials were flux weighted with a ^{235}U spectrum (Table D-4).

Table D-1. Detector Composition and Shielding

Monitors	Shielding	Reaction
11.87 U-Al	Cd-Ag 0.02676-inch Cd	$^{238}U(n,f)$
1.61% Np-Al	Cd-Ag 0.02676-inch Cd	$^{237}Np(n,f)$
Ni	Cd-Ag 0.02676-inch Cd	$^{58}Ni(n,p)^{58}Co$
0.66% Co-Al	Cd-0.040-inch Cd	$^{59}Co(n,\gamma)^{60}Co$
0.66% Co-Al	None	$^{59}Co(n,\gamma)^{60}Co$
Fe	None	$^{54}Fe(n,p)^{54}Mn$

Table D-2. Measured Detector Activities After Cycle 1

Monitor	Nuclide	Activity, μCi/g			
		OCI-FD5	OCI-FD6	OCI-FD7	OCI-FD8
^{238}U	^{103}Ru	8.70×10^{1}	6.80×10^{1}	6.91×10^{1}	5.06×10^{1}
	^{137}Cs	6.81×10^{-1}	1.15	1.57	1.07
	^{141}Ce	5.69×10^{1}	4.44×10^{1}	4.45×10^{1}	3.32×10^{1}
	^{144}Ce	3.31×10^{1}	$2.58 \quad 10^{1}$	2.59×10^{1}	1.97×10^{1}
	^{103}Ru	4.07×10^{2}	2.86×10^{2}	3.02×10^{2}	2.41×10^{2}
^{237}Np	^{137}Cs	1.09×10^{1}	7.76	7.95	6.39
	^{141}Ce	2.68×10^{2}	1.82×10^{2}	1.96×10^{2}	1.48×10^{2}
^{58}Na	^{144}Ce	1.52×10^{2}	1.03×10^{2}	1.10×10^{2}	8.94×10^{2}
	^{58}Co	9.61×10^{2}	7.33×10^{2}	7.27×10^{2}	5.64×10^{2}
$^{59}Co(Cd)$	^{60}Co	7.43×10^{3}	5.94×10^{3}	5.78×10^{3}	5.17×10^{3}
^{59}Co	^{60}Co	4.72×10^{4}	3.06×10^{4}	3.01×10^{4}	2.04×10^{4}
^{54}Fe	^{54}Mn	3.92×10^{2}	2.85×10^{2}	3.18×10^{2}	2.82×10^{2}

Table D-3. Measured Detector Activities After Cycle 2

Monitor	Post-irradiation wt, mg	Isotope	Total, μCi	Total, μCi/g	Reaction	Target, μCi/gm(a)
ED1						
^{238}U	47.00	^{95}Zr	2.047-1	4.36	$^{238}U(n,f)FP$	4.23+1
		^{95}Nb	5.017-1	1.07+1		1.04+2
		^{103}Ru	2.424-1	5.16		5.01+1
		^{137}Cs	9.01-3	1.92-1		1.86
		^{141}Ce	1.820-1	3.87		3.76+1
		^{106}Ru	6.685-2	1.42		1.38+1
		^{140}Ba	1.400-1	2.98		2.89+1
^{237}Np	79.44	^{95}Zr	2.911-1	3.66	$^{237}Np(n,f)FP$	2.54+2
		^{95}Nb	6.330-1	7.97		5.53+2
		^{103}Ru	2.998-1	3.77		2.62+2
		^{137}Cs	9.612-3	1.21-1		8.40
		^{140}Ba	1.805-1	2.27		1.58+2
		^{141}Ce	2.944-1	3.71		2.58+2
		^{106}Ru	6.904-2	8.69-1		6.03+1
Ni	133.22	^{58}Co	8.706+1	6.54+2	$^{58}Ni(n,p)^{58}Co$	9.35+2
		^{60}Co	2.313-1	1.74	$^{60}Ni(n,p)^{60}Co$	6.65
Co(Cd)	16.00	^{60}Co	1.002	6.26+1	$^{59}Co(n,\gamma)^{60}Co$	9.48+3
Fe	151.66	^{54}Mn	4.673	3.08+1	$^{54}Fe(n,p)^{54}Mn$	5.29+2
		^{59}Fe	9.230	6.09+1	$^{58}Fe(n,\gamma)^{59}Fe$	1.85+4
Co	15.70	^{60}Co	7.601	4.84+2	$^{59}Co(n,\gamma)^{60}Co$	7.33+4
ED2						
^{238}U	55.74	^{95}Zr	3.268-1	5.86	$^{238}U(n,f)FP$	5.69+1
		^{95}Nb	7.841-1	1.41+1		1.37+2
		^{103}Ru	3.864-1	6.93		6.73+1
		^{137}Cs	1.14-2	2.05-1		1.99
		^{140}Ba	2.464-1	4.42		4.29+1
		^{141}Ce	2.887-1	5.18		5.03+1
		^{106}Ru	9.383-2	1.68		1.63+1

Table D-3. (Cont'd)

Monitor	Post-irradiation wt, mg	Isotope	Total, μCi	Total, μCi/g	Reaction	Target, μCi/gm[a]
^{237}Np	84.2	^{95}Zr	3.590-1	4.26	$^{237}Np(n,f)FP$	2.96+2
		^{95}Nb	7.387-1	8.77		6.09+2
		^{103}Ru	3.677-1	4.37		3.03+2
		^{137}Cs	1.169-2	1.39-1		9.65
		^{140}Ba	2.276-1	2.70		1.88+2
		^{141}Ce	3.648-1	4.33		3.01+2
		^{144}Ce	1.898-1	2.25		1.56+2
		^{106}Ru	7.255-2	8.62-1		5.99+1
Ni	136.03	^{58}Co	1.106+2	8.13+2	$^{58}Ni(n,p)^{58}Co$	1.20+3
		^{60}Co	2.301-1	1.69	$^{60}Ni(n,p)^{60}Co$	6.46
Co(Cd)	18.75	^{60}Co	1.306	6.97+1	$^{59}Co(n,\gamma)^{60}Co$	1.06+4
Fe	154.44	^{54}Mn	5.549	3.59+1	$^{54}Fe(n,p)^{54}Mn$	6.17+2
		^{59}Fe	1.314+1	8.51+1	$^{58}Fe(n,\gamma)^{59}Fe$	2.58+4
Co	16.72	^{60}Co	8.984	5.37+2	$^{59}Co(n,\gamma)^{60}Co$	8.14+4
ED3						
^{238}U	50.1	^{95}Zr	1.756-1	3.51	$^{238}U(n,f)FP$	3.41+1
		^{95}Nb	3.507-1	7.00		6.79+1
		^{103}Ru	2.043-1	4.08		3.96+1
		^{137}Cs	8.91-3	1.78-1		1.72
		^{140}Ba	1.369-1	2.73		2.65+1
		^{141}Ce	1.615-1	3.22		3.12+1
		^{106}Ru	6.272-2	1.25		1.21+1
^{237}Np	82.66	^{95}Zr	2.323-1	2.81	$^{237}Np(n,f)FP$	1.95+2
		^{95}Nb	4.579-1	5.54		3.85+2
		^{103}Ru	2.372-1	2.87		1.99+2
		^{137}Cs	708-3	1.17-1		8.13
		^{140}Ba	1.819-1	2.20		1.53+2
		^{141}Ce	2.423-1	2.93		2.03+2
		^{106}Ru	4.977-2	6.02-1		4.18+1
Ni	128.29	^{58}Co	6,422+1	5.01+2	$^{58}Ni(n,p)^{58}Co$	7.39+2
		^{60}Co	2.006-1	1.56	$^{60}Ni(n,p)^{60}Co$	5.96

Table D-3. (Cont'd)

Monitor	Post-irradiation wt, mg	Isotope	Total, μCi	Total, μCi/g	Reaction	Target, μCi/gm(a)
Co(Cd)	20.28	^{60}Co	1.269	6.26+1	$^{59}Co(n,\gamma)^{60}Co$	9.48+3
Fe	150.81	^{54}Mn	3.904	2.59+1	$^{54}Fe(n,p)^{54}Mn$	4.45+2
		^{59}Fe	5.308	3.52+1	$^{58}Fe(n,\gamma)^{59}Fe$	1.07+4
Co	16.88		6.529	3.87+2	$^{59}Co(n,\gamma)^{60}Co$	5.86+4
ED4						
^{238}U	52.92	^{95}Zr	2.509-1	4.74	$^{238}U(n,f)FP$	4.60+1
		^{95}Nb	6.527-1	1.23+1		1.19+2
		^{103}Ru	2.921-1	5.52		5.36+1
		^{137}Cs	1.20-2	2.27-1		2.20
		^{141}Ce	2.250-1	4.25		4.12+1
		^{106}Ru	1.031-1	1.95		1.89+1
^{237}Np	69.22	^{95}Zr	2.522-1	3.64	$^{237}Np(n,f)FP$	2.53+2
		^{95}Nb	5.967-1	8.62		5.99+2
		^{103}Ru	2.524-1	3.65		2.53+2
		^{137}Cs	1.11-2	1.60-1		1.11+1
		^{141}Ce	2.502-1	3.61		2.51+2
		^{144}Ce	1.368-1	1.98		1.38+2
		^{106}Ru	6.397-2	9.24-1		6.42+1
Ni	129.20	^{58}Co	8.734+1	6.76+2	$^{58}Ni(n,p)^{58}Co$	9.97+2
		^{60}Co	2.238-1	1.73	$^{60}Ni(n,p)^{60}Co$	6.61
Co(Cd)	20.25	^{60}Co	1.331	6.57+1	$^{59}Co(n,\gamma)^{60}Co$	9.95+3
Fe	154.27	^{54}Mn	4.978	3.23+1	$^{54}Fe(n,p)^{54}Mn$	5.55+2
		^{59}Fe	1.013+1	6.57+1	$^{58}Fe(n,\gamma)^{59}Fe$	1.99+4
Co	16.46	^{60}Co	8.518	5.18+2	$^{59}Co(n,\gamma)^{60}Co$	7.85+4

(a) The following abundance and weight percents were used to calculate the disintegration rate per gram of target:

1. ^{238}U: 10.38 wt %; 99.27% isotopic.
2. ^{237}Np: 1.44 wt %; 100% isotopic.
3. Ni: 100%; ^{58}Ni 67.77% isotopic; ^{60}Ni 26.16% isotopic.
4. Co: 0.66 wt %; ^{59}Co 100% isotopic.
5. Fe: 100%; ^{54}Fe 5.82% isotopic; ^{58}Fe 0.33% isotopic.

Table D-4. Dosimeter Activation Cross Sections[a]

G	Energy range, MeV		^{237}Np	^{238}U	^{58}Ni	^{54}Fe
1	13.3	-15.0	2.231	1.073	0.460	0.425
2	10.0	-12.2	2.34	0.981	0.622	0.537
3	8.18	-10.0	2.31	0.991	0.659	0.583
4	6.36	-8.18	2.09	0.917	0.638	0.572
5	4.96	-6.36	1.54	0.60	0.54	0.473
6	4.06	-4.96	1.53	0.562	0.403	0.325
7	3.01	-4.06	1.616	0.553	0.264	0.206
8	2.46	-3.01	1.69	0.550	0.139	0.096
9	2.35	-2.46	1.695	0.553	0.089	0.0524
10	1.83	-2.35	1.676	0.535	0.051	0.022
11	1.11	-1.83	1.593	0.229	0.0128	0.0115
12	0.55	-1.11	1.217	0.008	0.00048	--
13	0.111	-0.55	0.1946	0.00013	--	--
14	0.0033	-0.111	0.0410	--	--	--

[a] ENDF/B4 values flux weighted with a fission spectrum.